BROOKHAVEN
NATIONAL LABORATORY

BNL-81651-2008

BNL-GFR-2007-001

managed by Brookhaven Science Associates
for the U.S. Department of Energy

ATWS Transients for the 2400 MWt Gas-Cooled Fast Reactor

Lap-Yan Cheng, Hans Ludewig

August 5, 2007

Energy Sciences and Technology Department

Brookhaven National Laboratory
P.O. Box 5000
Upton, NY 11973-5000
www.bnl.gov

DISCLAIMER

TABLE OF CONTENTS

LIST OF FIGURES

LIST OF FIGURES (CONT'D)

FIGURE **Page**

LIST OF TABLES

1.0 Introduction

Reactivity transients have been analyzed with an updated RELAP5-3D (ver. 2.4.2) system model of the pin core design for the 2400MWt gas-cooled fast reactor (GCFR). Additional reactivity parameters were incorporated in the RELAP5 point-kinetics model to account for reactivity feedbacks due to axial and radial expansion of the core, fuel temperature changes (Doppler effect), and pressure changes (helium density changes). Three reactivity transients without scram were analyzed and the incidents were initiated respectively by reactivity ramp, loss of load, and depressurization. During the course of the analysis the turbine bypass model for the power conversion unit (PCU) was revised to enable a better utilization of forced flow cooling after the PCU is tripped. The analysis of the reactivity transients demonstrates the significant impact of the PCU on system pressure and core flow. Results from the modified turbine bypass model suggest a success path for the GCFR to mitigate reactivity transients without scram.

2.0 Modifications to RELAP5-3D Model

The latest pin core design of the 2400MWt GCFR is described in Ref. [1]. The RELAP5 model used in the previous accident analysis [2, 3] of the 2400 MWt GCFR was based on the vertical split segment pin geometry [1] with an active core height of 1.34m and a total pin length of 3.34m. In the latest design the fuel pellets were changed to annular shape with a central void region. Table 1 provides the reference geometry for the pin design.

Table 1. Reference Pin Geometry

2400 MWt PIN CORE	
Fuel Assembly Geometry	
Flat-to-flat of hexagonal duct (outside), mm	215
Duct wall thickness, mm	3.7
Interassembly gap, mm	7
Number of pins per core subassembly	271
Number of rings (excluding center one)	9
Number of spacers	3
Hydraulic diameter, mm	12.2
Pin pitch (average), mm	12.6
Fuel Pin Geometry	
Total pin length, m	3.34
Fuel pellet diameter, ID/ODmm (annular)	3.02/7.37
Fuel clad thickness, mm	1.0
Fuel pin diameter, mm	9.57

The core layout, as shown in Figure 1, consists of a central region of fuel assemblies surrounded by concentric regions of reflector assemblies and shield assemblies. In the fueled region there are 366 fuel assemblies, 54 fuel assemblies with control rods, and 7

fuel assemblies with shutdown rods. The reflector and shield regions each consists of 174 reflector assemblies and 318 shield assemblies respectively.

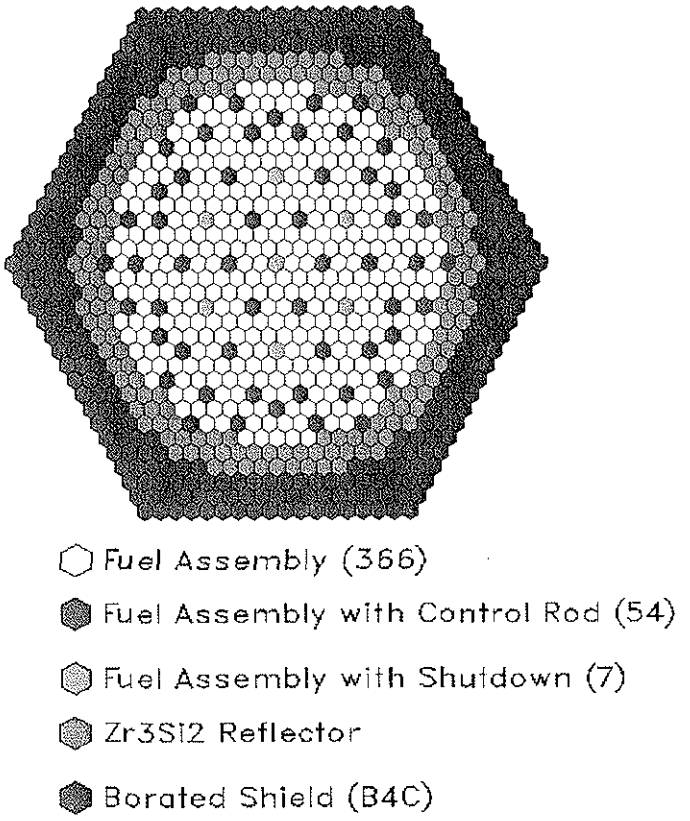

Figure 1. 2400 MWt backup pin core reference layout.

As discussed in [2] the fuel assemblies were grouped into three types of core channels, hot assembly, hot zone, and average zone. The power fraction in each channel type is shown in Table 2 together with the corresponding radial power factor, normalized to the core average assembly power.

Table 2. Core Channel Power Distribution

3 Core Channels			
	Hot Assembly	Hot Zone	Average Zone
Regular Assembly	6	48	312
Control Assembly	0	7	54
Number of Fuel Pins	1626	14646	97188
Power Fraction	1.88%	15.6%	82.5%
Radial Power Factor	1.31	1.21	0.963

The RELAP5 model from Ref. [2, 3] was modified to reflect changes in the heat structures for the fuel assemblies (the number of assemblies in the average zone was corrected). The three changes are:

1. Change fuel pellets from cylindrical to annular shape.
2. Update power faction in each core channel type.
3. Update view factors (used in radiative heat transfer calculations) based on changes in surface areas.

3.0 Modeling of Reactivity Feedbacks

ANL [4] provided the 6-group precursor decay constants for both BOC and EOC conditions. The precursor fractions (β_i), decay constants, and prompt neutron lifetime (λ) are summarized in Table 3.

Table 3. Delayed Neutron Group Constants

	Beginning of Cycle (BOC)			End of Cycle (EOC)		
Group	β_i	β_i/β	Decay Constant, s^{-1}	β_i	β_i/β	Decay Constant, s^{-1}
1	7.7368×10^{-5}	0.02246	0.01341	7.6578×10^{-5}	0.02260	0.01341
2	6.0356×10^{-4}	0.17524	0.03090	5.9977×10^{-4}	0.17698	0.03088
3	5.0247×10^{-4}	0.14589	0.11814	4.9524×10^{-4}	0.14613	0.11802
4	1.248×10^{-3}	0.36235	0.31053	1.2255×10^{-3}	0.36161	0.31024
5	7.374×10^{-4}	0.21410	0.88613	7.2285×10^{-4}	0.21329	0.88564
6	2.754×10^{-4}	0.07996	2.96420	2.6907×10^{-4}	0.07939	2.96220
β	0.00344422			0.00338902		
λ	7.59227×10^{-7} s			7.20510×10^{-7} s		
β/λ	4.53648×10^{3} s^{-1}			4.70364×10^{3} s^{-1}		

The above parameters are used as inputs to the point kinetics model in RELAP5 for the GCFR.

A set of reactivity coefficients have been developed from the core neutronics design presented in [1] to account for reactivity feedbacks from temperature and pressure changes in the course of a transient. For the present analyses the reactivity coefficients are derived from safety parameters given in Table 2.3 of Ref. [1] for the split-batch core under end of equilibrium cycle conditions. The derivation of the reactivity coefficients are discussed in the following sub-sections.

3.1 Depressurization Reactivity

Upon depressurization the helium density in the core decreases and that leads to a hardening of the neutron spectrum resulting in a positive reactivity effect. According to Ref. [1] the 1.15$ positive reactivity change due to depressurization was calculated by an instantaneous isothermal depressurization from the operating pressure to atmospheric pressure, i.e. from 70 bars to 1 bar. The change in helium density can be represented by a change in the mass of helium in the active core. From a steady-state RELAP5 run the mass of helium occupying the free volume inside the fuel assemblies in the fueled region

is 37.0081 kg. The corresponding mass at 1 bar is 37.0081/70 kg. Thus a depressurization coefficient in terms of helium mass can be expressed as,

Depressurization reactivity coefficient
= 1.15\$ / (37.0081 – 37.0081/70) kg
= 3.1525×10^{-2} \$/kg

Reactivity feedback due to depressurization
= 3.1525×10^{-2} \$/kg x $(M_0 - M_1)$,

where, M_0 is the initial mass of helium in the active core and M_1 is the transient mass of helium in the active core.

In RELAP5 the reactivity feedback is calculated in \$ and a control variable is defined to calculate the mass of helium (in kg) occupying the free volume inside the fuel assemblies in the fueled region of the core.

3.2 Doppler Reactivity

The Doppler effect results in a negative reactivity due to an increase in the fuel temperature. According to Ref. [1] the Doppler coefficient is -0.28 ¢/K. A RELAP5 control variable is defined to calculate the volume-averaged fuel temperature in the active core. This is an average temperature of the annular fuel and it includes all three types of core channel, hot assembly, hot zone, and average zone.

Reactivity feedback due to Doppler effect
= -0.28×10^{-2}\$/K x $(T_{f1} - T_{f0})$,

where, T_{f0} is the initial averaged fuel temperature (in K) and T_{f1} is the transient averaged fuel temperature.

3.3 Axial Expansion Reactivity

According to Ref. [1] axial thermal expansion of the fuel pellets results in a negative reactivity and the reactivity coefficient is -0.13 \$/cm. The axial expansion of the fuel is calculated as,

$\Delta L = \alpha_f L \Delta T_f$,

where,
L = active core height = 1.347 m
α_f = thermal expansion coefficient = 11.9×10^{-6}/K (this is a mean coefficient for uranium carbide in the temperature range 25 – 1000°C [5])
ΔT_f = average fuel temperature change in deg. K = $(T_{f1} - T_{f0})$

Reactivity feedback due to axial expansion
$= -0.13$ \$/cm x 100cm/m x 11.9×10^{-6}/K x 1.347 m x $(T_{f1} - T_{f0})$
$= -2.0838 \times 10^{-4}$ \$/K x $(T_{f1} - T_{f0})$

3.4 Radial Expansion Reactivity

The fuel assemblies sit in a grid plate structure and the radial movement of the core is due to thermal expansion of the grid plate. However the current RELAP5 model does not have a heat structure representing the grid plate and the core radial expansion is instead approximated by the radial expansion of the fuel assembly can. According to Ref. [1] radial thermal expansion of the core results in a negative reactivity and the reactivity coefficient is -0.41 \$/cm. The radial expansion of the core is calculated as,

$\Delta D = \alpha_c D \Delta T_c$,

where,
D= active core diameter = 4.75 m [1]
α_c = thermal expansion coefficient = 5.32×10^{-6}/K (this is the linear expansion coefficient for the assembly can made of Hexoloy silicon carbide in the temperature range 700 – 2000°C [6])
ΔT_c = average assembly can temperature change in deg. K = $(T_{c1} - T_{c0})$
T_{c0} = initial averaged assembly can temperature
T_{c1} = transient averaged assembly can temperature

A RELAP5 control variable is defined to calculate the volume-averaged assembly can temperature in the active core. This is an average temperature of the fuel assembly cans and it includes all three types of core channel, hot assembly, hot zone, and average zone.

Reactivity feedback due to radial expansion
$= -0.41$ \$/cm x 100cm/m x 5.32×10^{-6}/K x 4.75 m x $(T_{c1} - T_{c0})$
$= -1.0361 \times 10^{-3}$ \$/K x $(T_{c1} - T_{c0})$

In the RELAP5 analysis the four reactivity feedbacks are input as reactivity changes at every time step with all four feedbacks sum to zero at time zero. The reactivity coefficients as implemented in RELAP5 are summarized in Table 4.

Table 4. Reactivity Coefficients

	From Table 2.3 of Ref. [1]	RELAP5 Reactivity Feedback
Depressurization	1.15\$	3.1525×10^{-2}\$/kg $(M_0 - M_1)$
Doppler Effect	-0.28 ¢/K	-0.28×10^{-2}\$/K $(T_{f1} - T_{f0})$
Axial Expansion	-0.13 \$/cm	-2.0838×10^{-4}\$/K $(T_{f1} - T_{f0})$
Radial Expansion	-0.41 \$/cm	-1.0361×10^{-3}\$/K $(T_{c1} - T_{c0})$

4.0 Reactivity Transients

The updated RELAP5-3D system model of the GCFR was used to analyze three reactivity transients without scram. The reactivity transients are initiated by reactivity ramp, loss of load, and depressurization. In the process of analyzing the transients several parametric studies were made and they included reducing the reactivity coefficient of depressurization, modulating the operation of the turbine bypass valve, and reconfiguring the turbine bypass line.

4.1 Reactivity Ramp

A simple case of reactivity ramp was used to exercise the new model set up to analyze reactivity transients. Reactivity was inserted at a rate of 0.02$/s for 9.75s (a total of 0.195$). A scram signal was generated at 115% power but the reactor stayed on line while the electrical generator and PCU were tripped. Disengaging the generator created a load imbalance and the shaft of the PCU started to speed up. The over-speed was controlled by opening the turbine bypass valve, allowing high pressure helium flow to reach the outlet of the turbine. The increase in outlet pressure reduced the output of the turbine thus slowing down the rotating machinery of the PCU. In response to the redirection of the high pressure helium flow the whole system experienced a rapid drop in pressure due to pressure equalization inside the PCU. The reactor power showed a rapid increase due to the positive reactivity feedback from depressurization before turning around by negative reactivity feedbacks from Doppler and thermal expansion of the core. With the rapid increase in power the fuel reached the 1600°C safety limit in less than 2 seconds after PCU trip. The transient response of some of the system parameters are shown in the following figures.

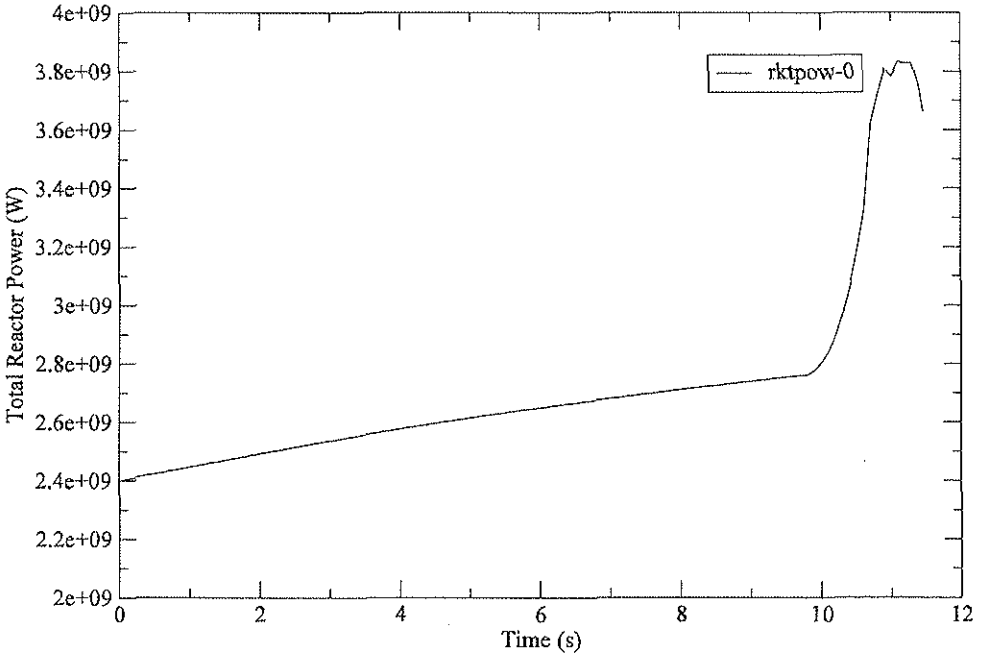

Figure 2. Reactor power, reactivity ramp.

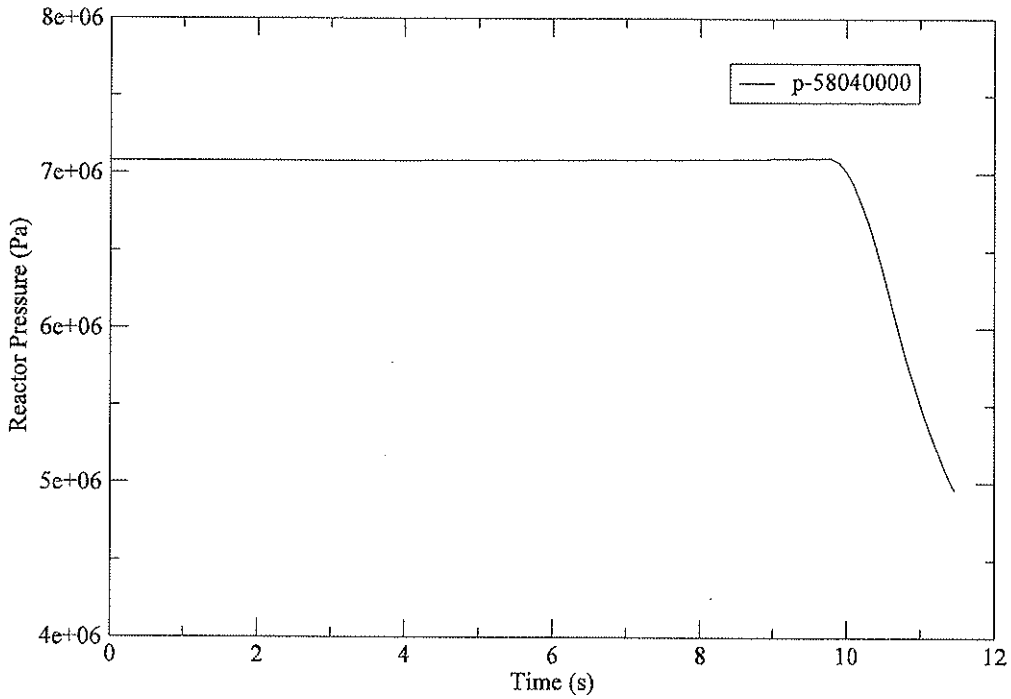

Figure 3. Reactor pressure, reactivity ramp.

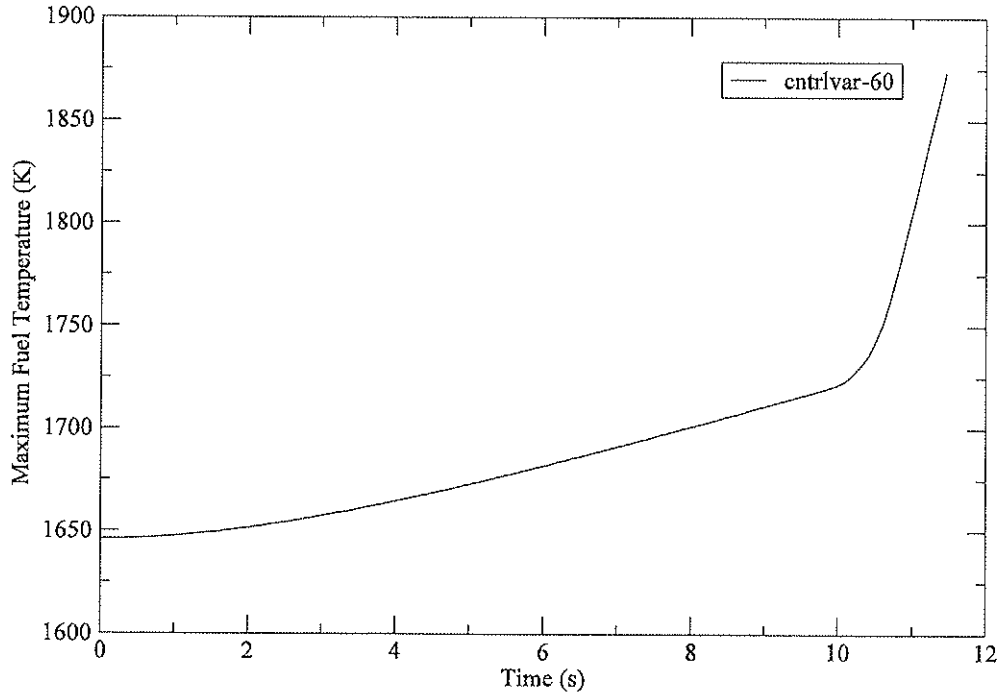

Figure 4. Maximum fuel temperature, reactivity ramp.

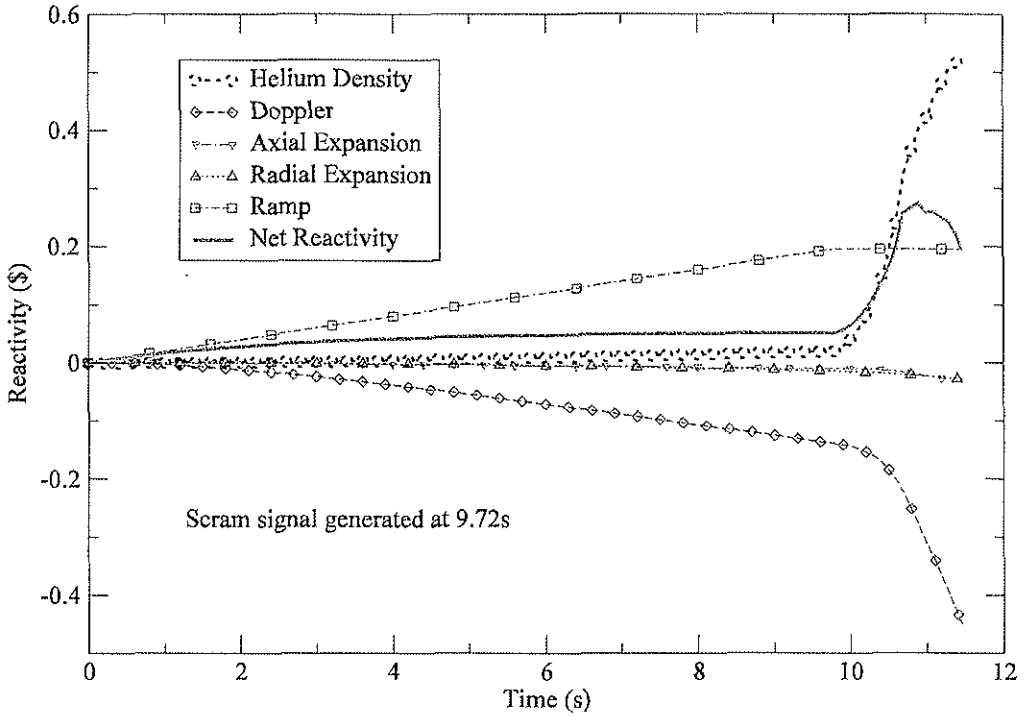

Figure 5. Reactivities as a function of time, reactivity ramp.

4.2 Loss of Load

It is clear from the result of the reactivity ramp accident that the depressurization reactivity feedback is the driving force behind the power increase in this transient when the reactor did not scram while the PCU turbine bypass system was activated to mitigate the over-speed of the turbomachinery. In order to isolate the reactivity effect of the depressurization a loss of load transient was analyzed. For the case of no reactor scram this transient was initiated by a loss of electrical load that led directly to an activation of the turbine bypass system. The ensuing pressure decrease would cause a positive reactivity addition and a corresponding power increase. The sensitivity of the power increase to the feedback coefficient was evaluated by parametrically reducing the pressure reactivity coefficient to 75% and 50% of the nominal value shown in Table 4. Qualitatively the progression of the loss of load transient without scram is very similar to the post PCU trip behavior of the reactivity ramp transient analyzed earlier. The reduction in the depressurization reactivity coefficient was not enough by itself to mitigate the power increase to prevent an overheating of the fuel. All three cases (nominal coefficient, 75% nominal, and 50% nominal) resulted in the fuel reaching the 1600°C safety limit. The only difference between the cases is the timing of reaching the temperature limit, with the case of a lower reactivity coefficient taking a longer time for the fuel to reach the temperature limit.

In modeling the turbine bypass system in RELAP5, the bypass valves were modeled to open fully in one second after actuation. There was no control to modulate the flow of helium in the bypass system. A way to limit the depressurization associated with a PCU

trip would be to regulate the bypass flow. With a more controlled depressurization it is anticipated that the power increase would be limited.

4.2.1 New Turbine Bypass Valve Model

A simple valve control scheme is developed to test out the idea of a controlled depressurization. The turbine bypass valve was originally represented by a motor valve that operated either in the full close or full open position. In the new scheme the turbine bypass valve is represented by a servo valve that can vary the valve area according to a control variable. For the servo valve the area is assumed to vary linear with the normalized shaft speed. Two control variables are defined, normalized valve area, A_N, and normalized shaft speed, ω_N.

A_N = Area of valve / Area of full open valve
ω_N = shaft speed / nominal shaft speed.

The control scheme varies A_N between 0 and 1 when ω_N varies between 1 and 1.05 with $A_N = 0$ for $\omega_N < 1$ and $A_N = 1$ for $\omega_N > 1.05$.

The loss of load transient was re-analyzed with the new bypass valve control scheme and some of the system parameters are shown in the following figures. The figures compare the results for the old and new bypass valve model. The results are for a case where the depressurization reactivity coefficient was reduced to a value equal to 75% nominal.

Based on the new analysis the simple control scheme is able to reduce the system pressure decrease by almost 50% (see Figure 6) and reactor power (Figure 7), system pressure (Figure 6) and helium flow (see Figures 9 and 10) all achieved quasi-steady condition in a matter of seconds. The only problem is that there is still a mismatch between rector power and core flow and the fuel continues to heat up to the 1600°C limit in about 15s from the initiation of the accident (see Figure 8). The helium temperatures at core outlet and inlet, shown in Figures 11 and 12 respectively, show consistent behavior of a core not getting sufficient cooling.

Additional results for the case of the new bypass valve model are shown in Figures 13 to 19. The RELAP5 model of the GCFR system represents the power conversion system with two loops; one loop has one PCU and the other loop lumps three PCUs into one. The PCU shaft speed for the two loops is shown in Figure 13. The normalized turbine bypass valve flow area for the two loops is shown in Figure 14. Based on Figures 13 and 14 the behavior of the two PCU loops is almost identical. Figures 15 through 17 show the inputs for the calculation of the reactivity feedbacks. They are the averaged fuel temperature, the averaged assembly can temperature, and the averaged helium mass in the core. The individual reactivity from different feedback effect is shown in Figure 18. Figure 19 shows the helium flow rate at two different locations inside the single PCU. The difference in flow on the hot side of the recuperator and the turbine is the amount of flow that recirculates inside the PCU (via the open bypass line) thus reducing flow to the reactor with an accompanying decrease in core cooling.

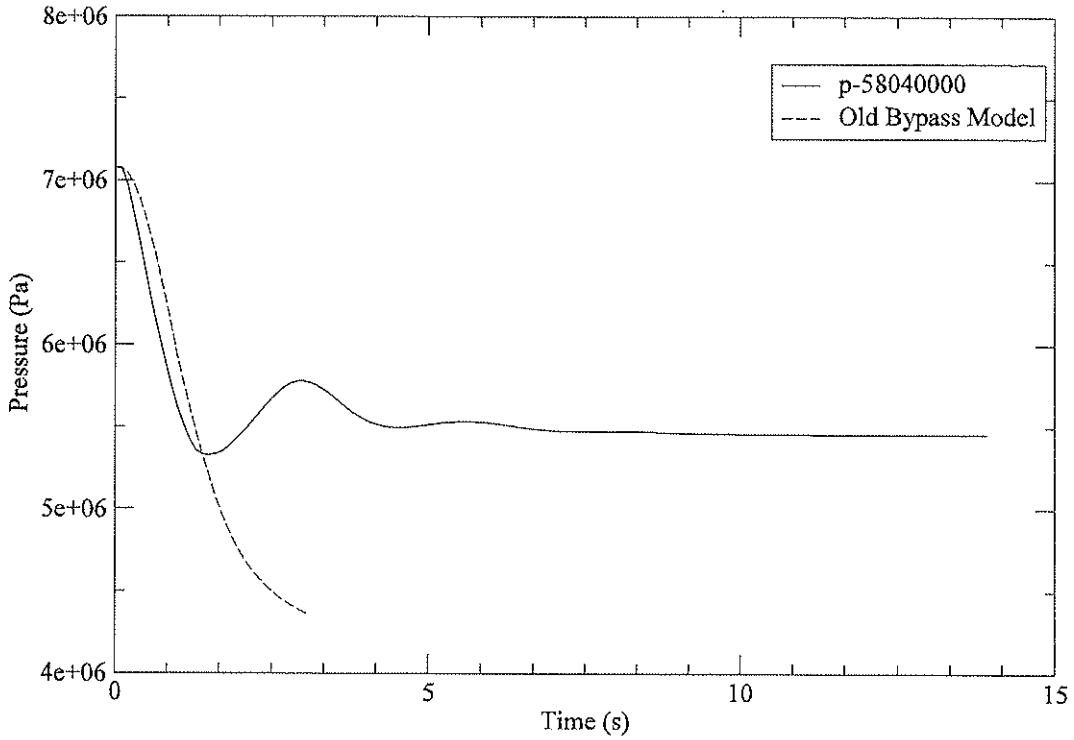

Figure 6. Reactor pressure, loss of load.

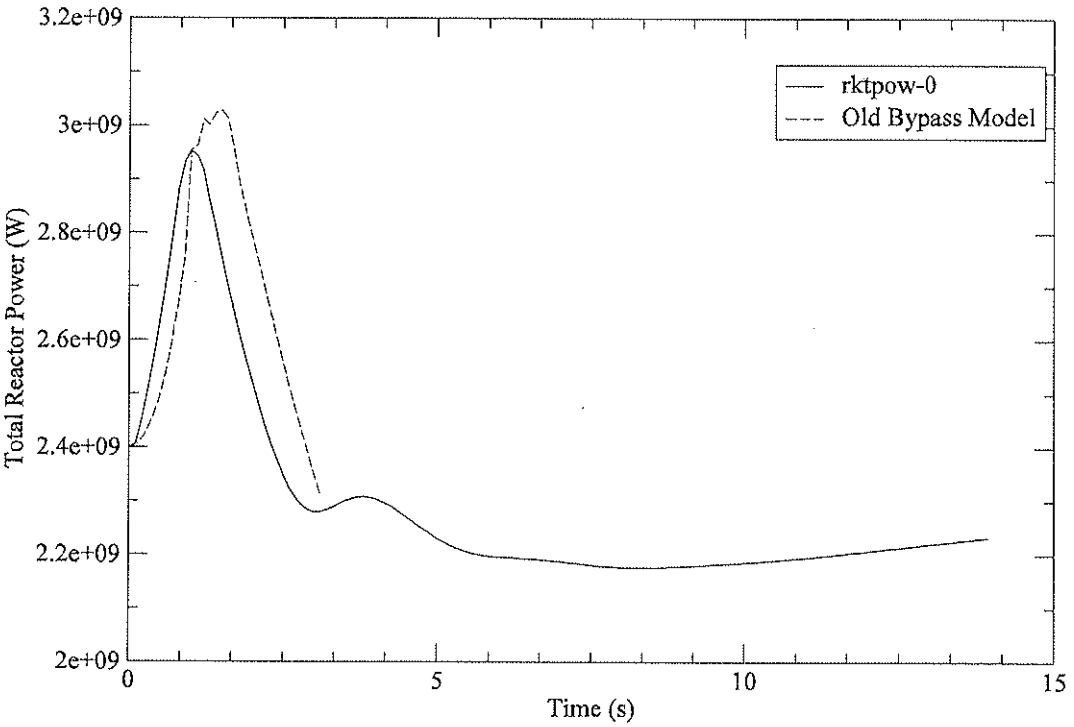

Figure 7. Reactor power, loss of load.

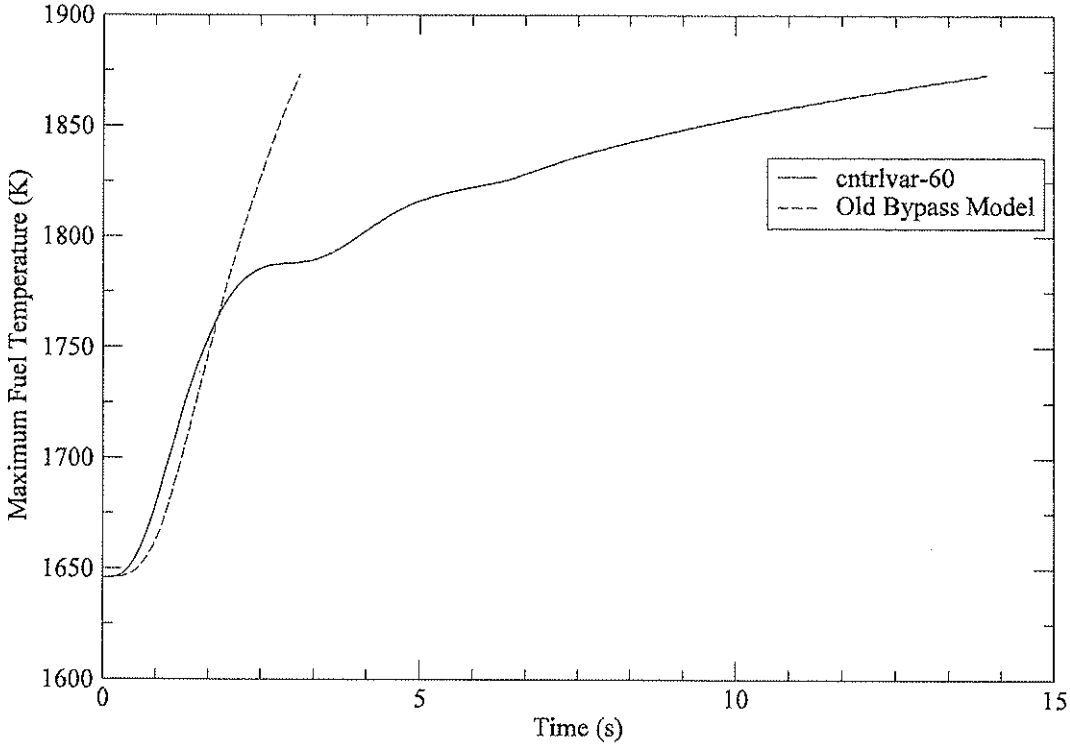

Figure 8. Maximum fuel temperature, loss of load.

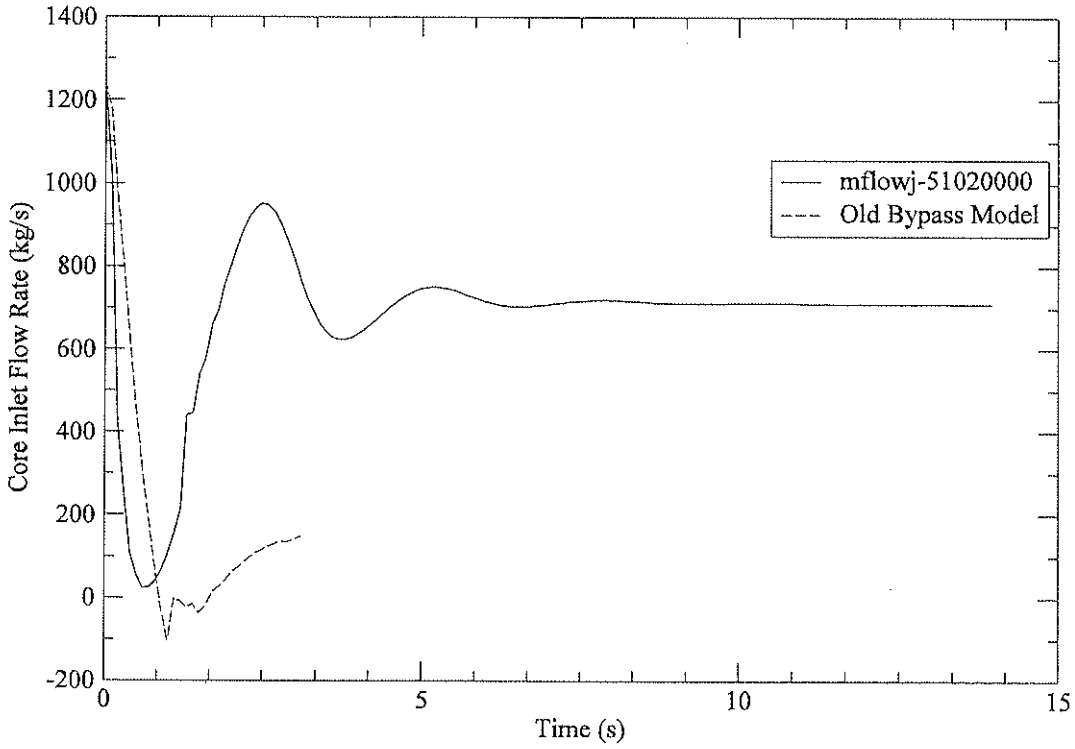

Figure 9. Helium flow rate at core inlet, loss of load.

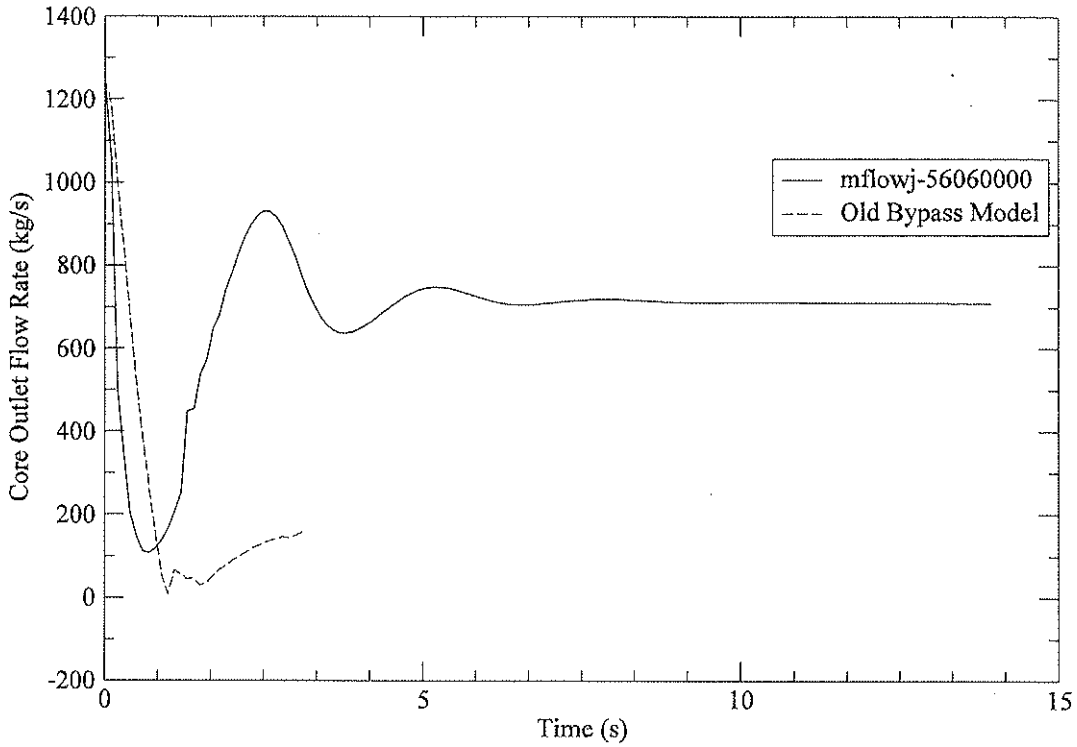

Figure 10. Helium flow rate at core outlet, loss of load.

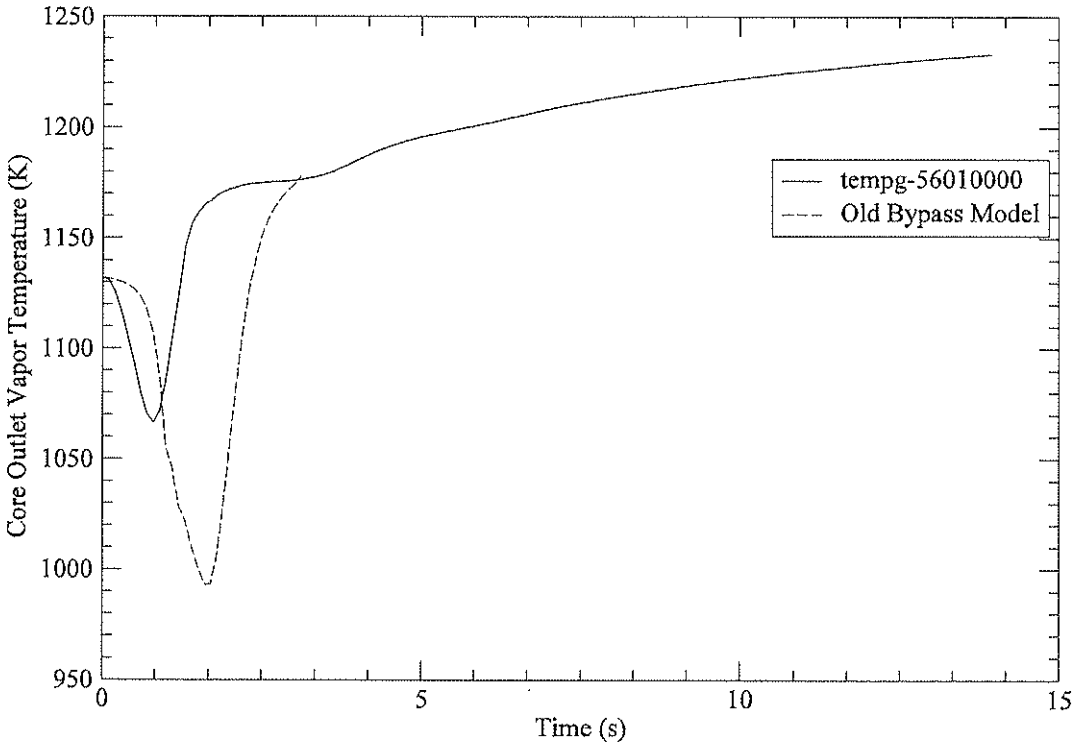

Figure 11. Helium temperature at core outlet, loss of load.

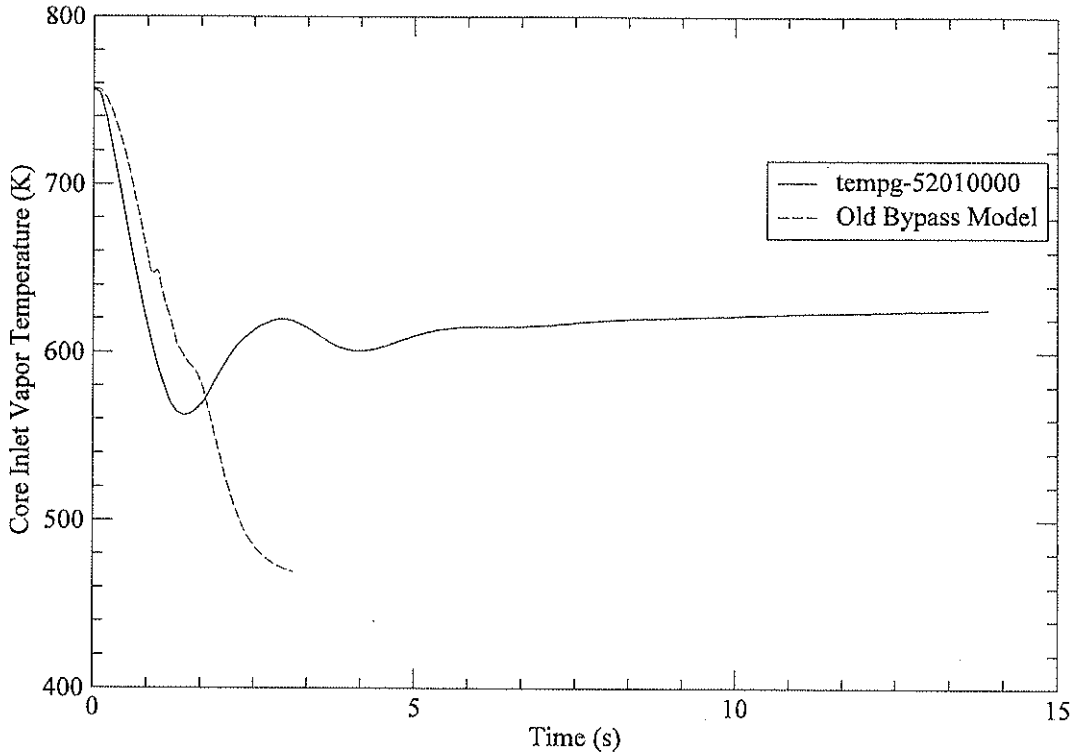

Figure 12. Helium temperature at core inlet, loss of load.

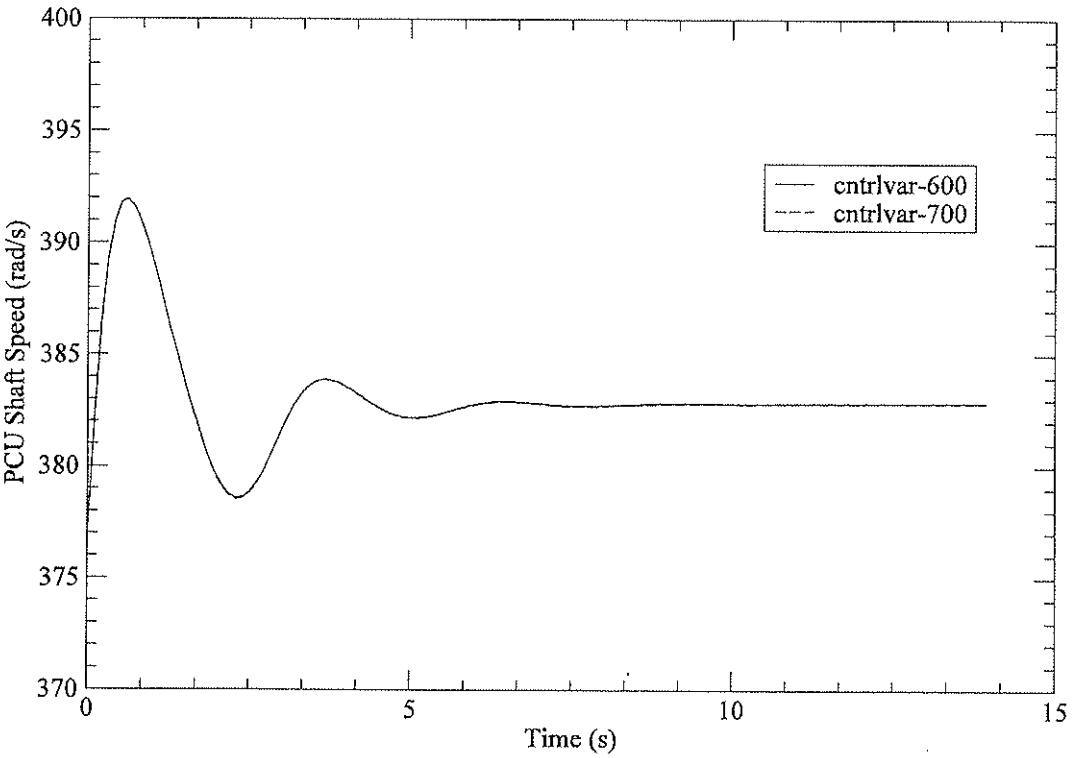

Figure 13. PCU shaft speed, new bypass valve model.

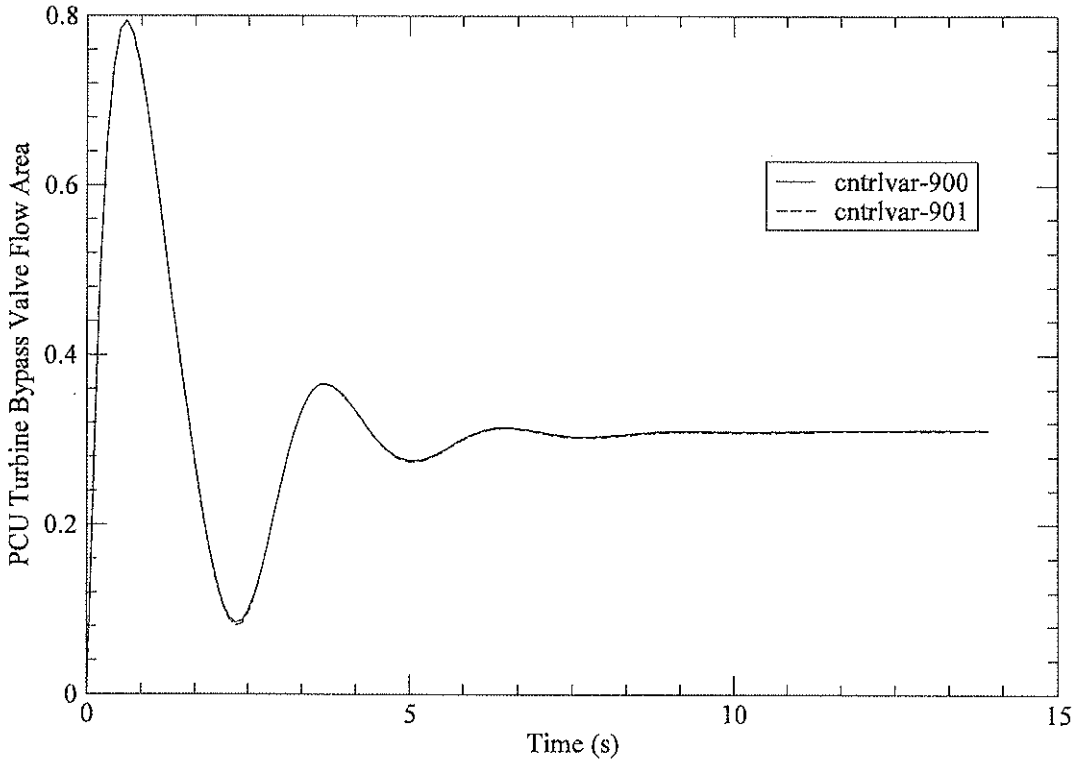

Figure 14. Normalized bypass valve flow area, loss of load.

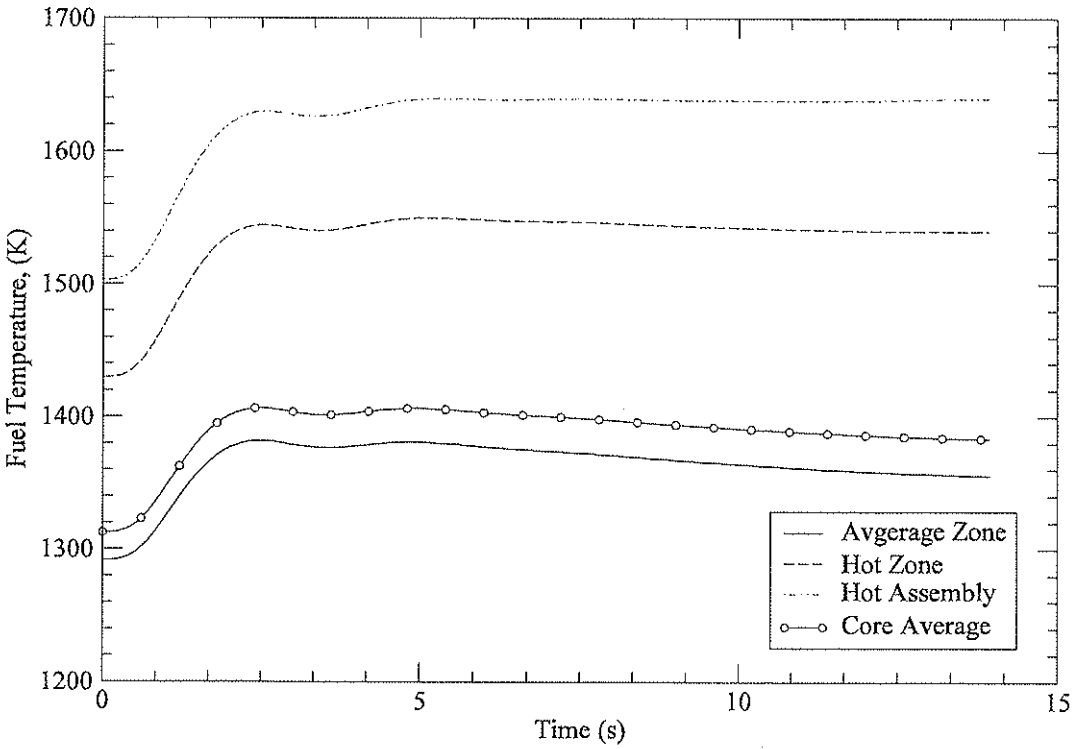

Figure 15. Volume-averaged fuel temperatures, loss of load.

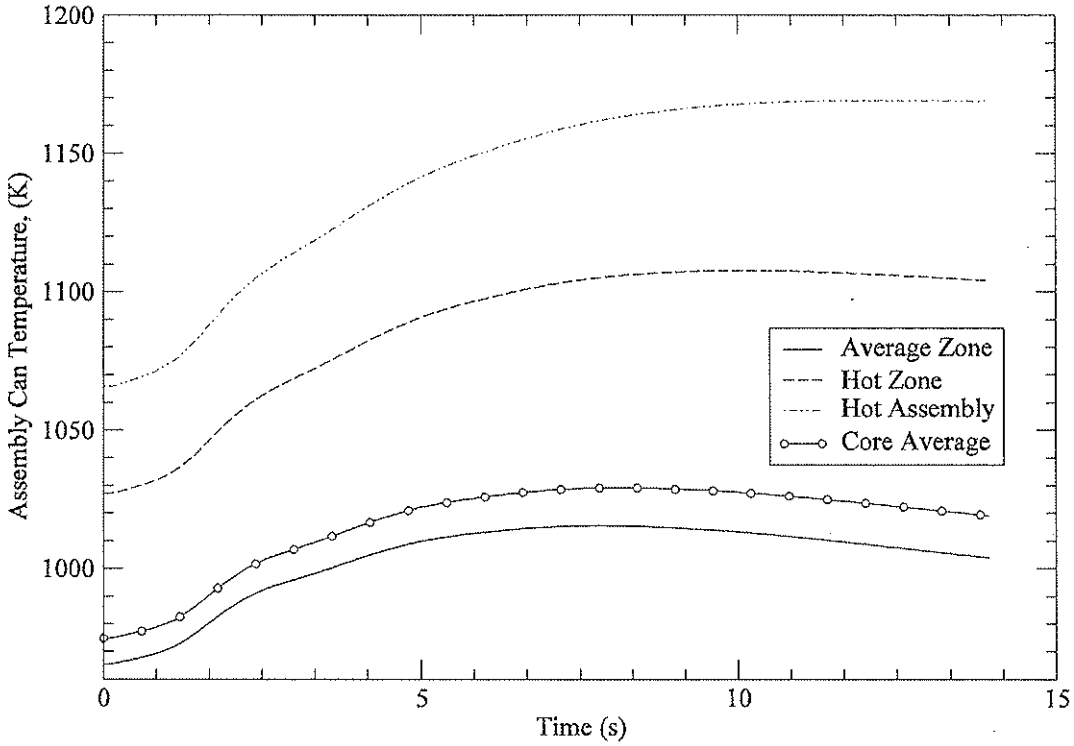

Figure 16. Volume-averaged assembly can temperature, loss of load.

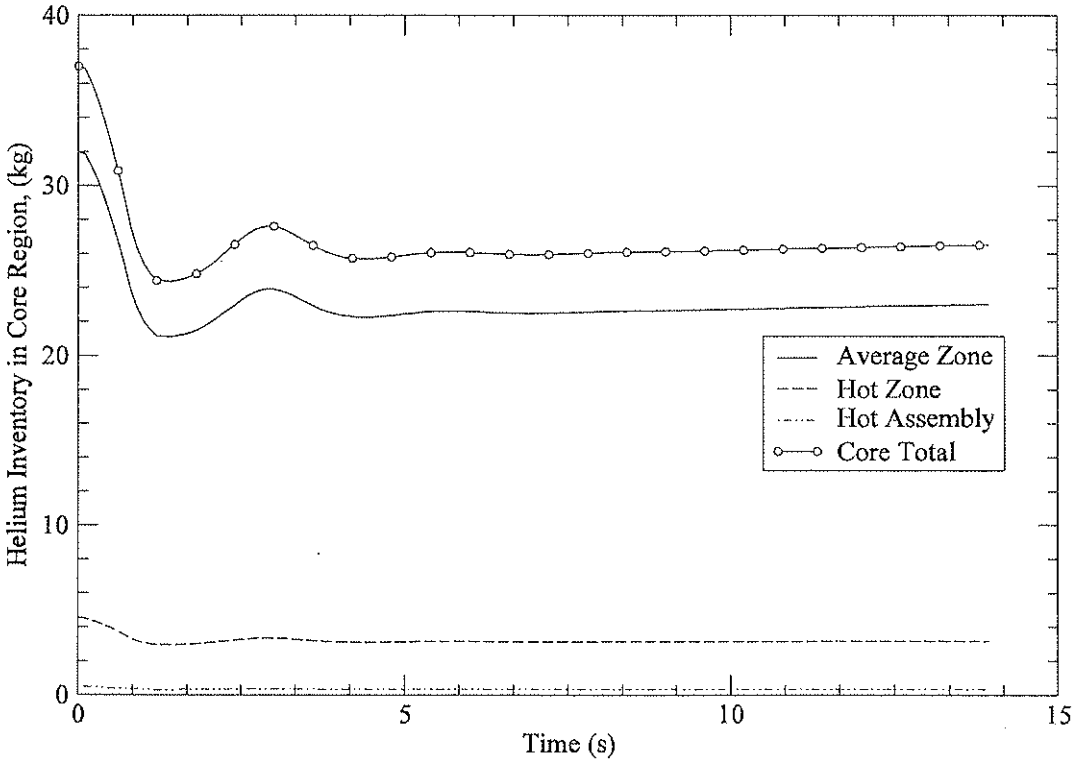

Figure 17. Helium inventory in the core, loss of load.

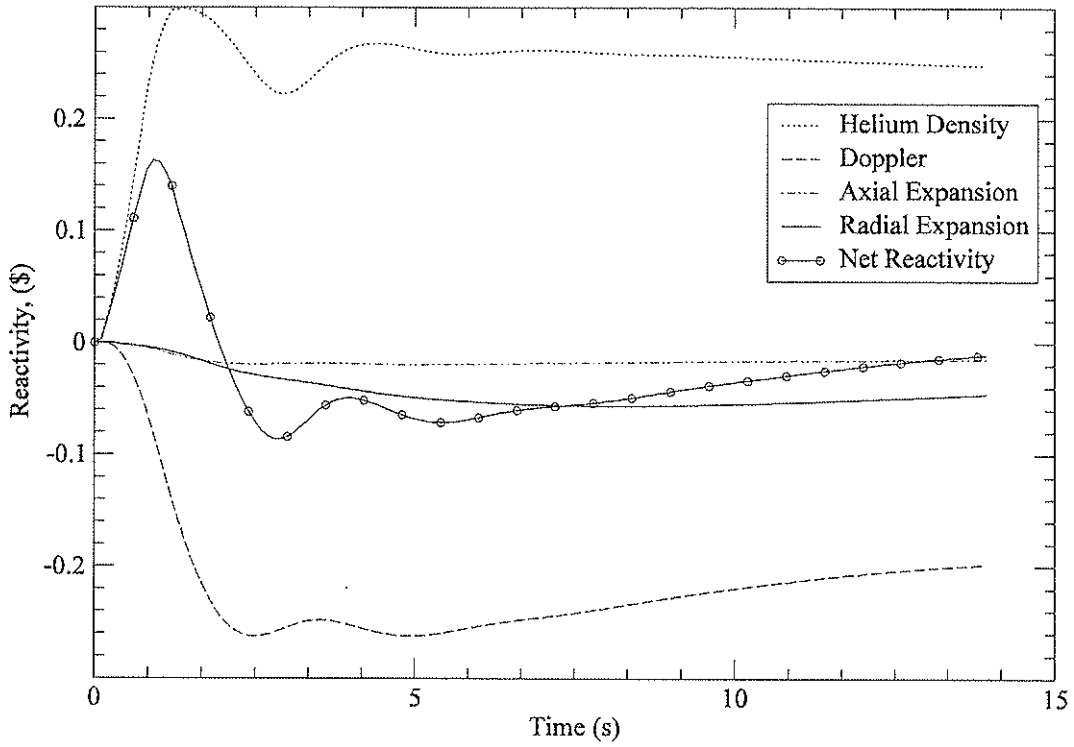

Figure 18. Reactivities for the new bypass valve model, loss of load.

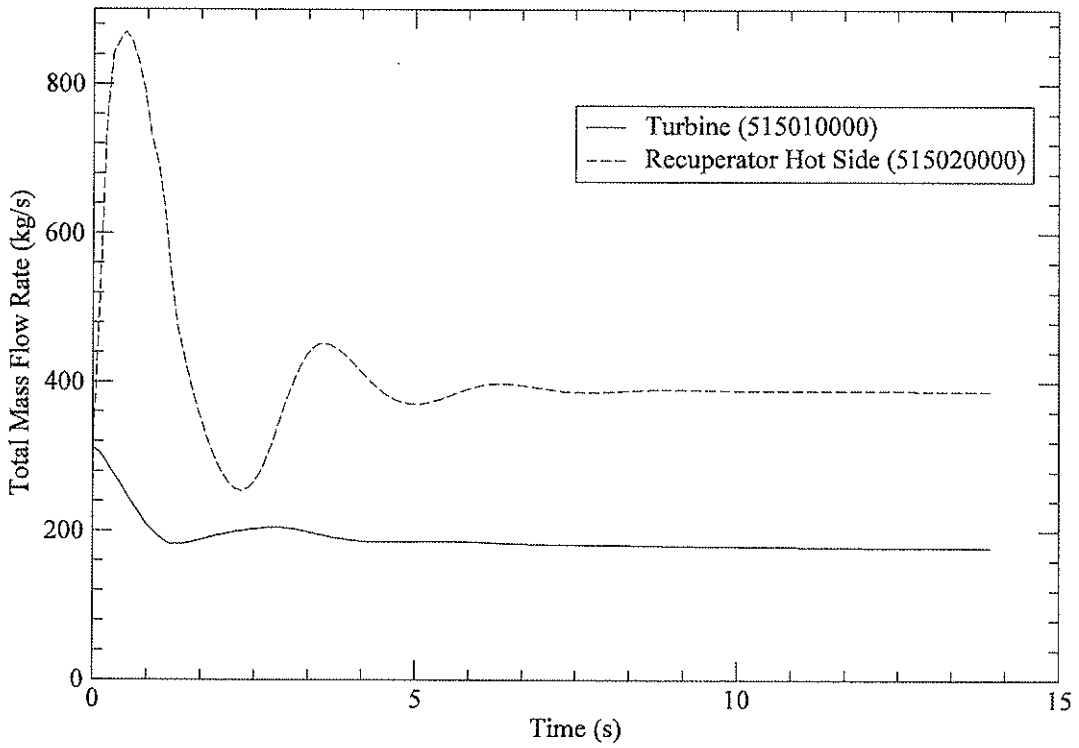

Figure 19. Helium mass flow rates, new bypass valve model, loss of load.

4.2.2 Reconfiguring the Turbine Bypass Line

The RELAP5 analyses have demonstrated the effectiveness of the turbine bypass system in preventing over-speeding of the turbomachinery. However the bypass line creates a flow path inside the PCU that short circuits some of the flow that is to be delivered to the reactor vessel. It is advantageous to avoid this short circuit and this can be accomplished by reconfiguring the bypass line. A new configuration is shown in Figure 20

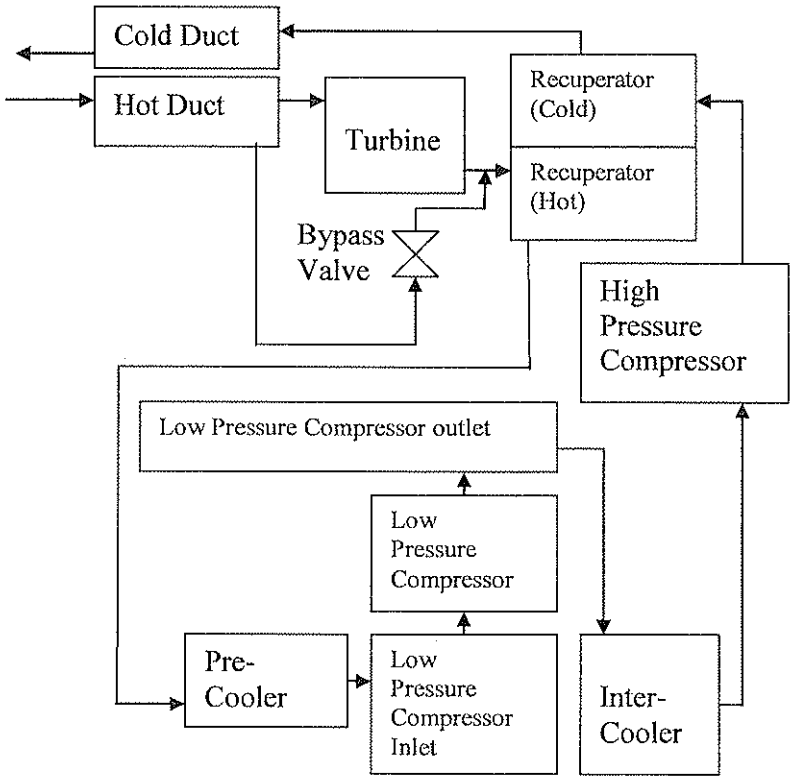

Figure 20. New configuration for the turbine bypass line.

The bypass line is now running parallel to the turbine, similar to the steam bypass system in LWRs. The bypass valve also will be regulated by the simple scheme discussed earlier. The new bypass line prevents over-speeding by diverting flow away from the turbine and thus reduces the output of the turbine.

A new loss of load transient is analyzed with the reconfigured bypass system. Results from the new and old configurations are plotted together for comparison in Figures 21 to 26. There are a number of similarities between the old and new results but one major difference makes all the difference in the outcome of the transient. Up to the end of the calculation (40s) there is no overheating of the fuel in the new analysis.

It is noted from Figure 20 that the upstream pressure of the new bypass configuration will be lower than the old one because the hot duct is at a lower pressure than the pressure at

the outlet of the high pressure compressor. The result is a slower and also lower depressurization for the new case (see Figure 21). The core flow is not only maintained in the new case but actually increased a little (see Figure 22). The spike in core flow right after PCU trip resulted in enhanced cooling and this can be seen in an initial drop in the maximum fuel temperature at the beginning of the transient (see Figure 23).The smaller rise in fuel temperature implies less negative reactivity to counteract the positive reactivity from depressurization. The net result is a bigger spike in power for the new case as compared to the old one (see Figure 24). The turbine flow rates (for one PCU), shown in Figure 25, for the old and new cases are about the same. Similar driving power is seen to produce similar flow in the PCU. This is observed in the flow on the hot side of the recuperator, shown in Figure 26. A crucial difference in Figure 26 between the old and new case is the flow on the cold side of the recuperator. For the new case flow on the hot and cold side is almost the same, indicating no internal recirculation. For the old case, flow on the cold side is lower than that on the hot side, indicating internal recirculation.

Initial results from the new bypass configuration are encouraging and the remaining reactivity transient, namely a depressurization accident, will be analyzed using this new model.

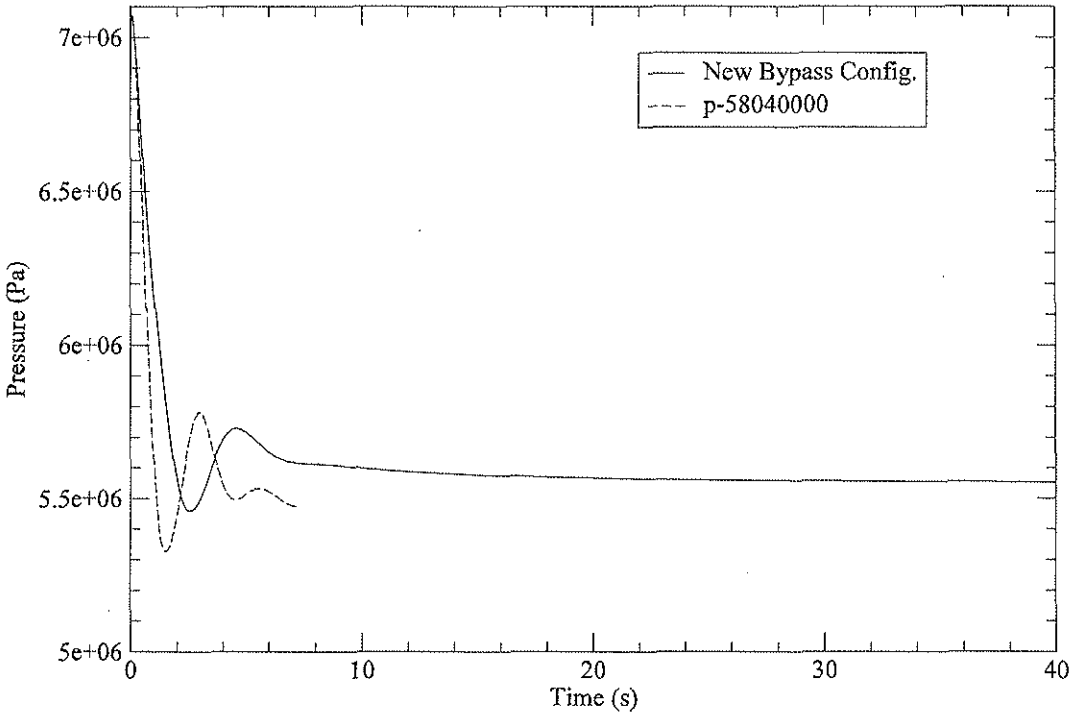

Figure 21. Reactor pressure, old & new bypass line model, loss of load.

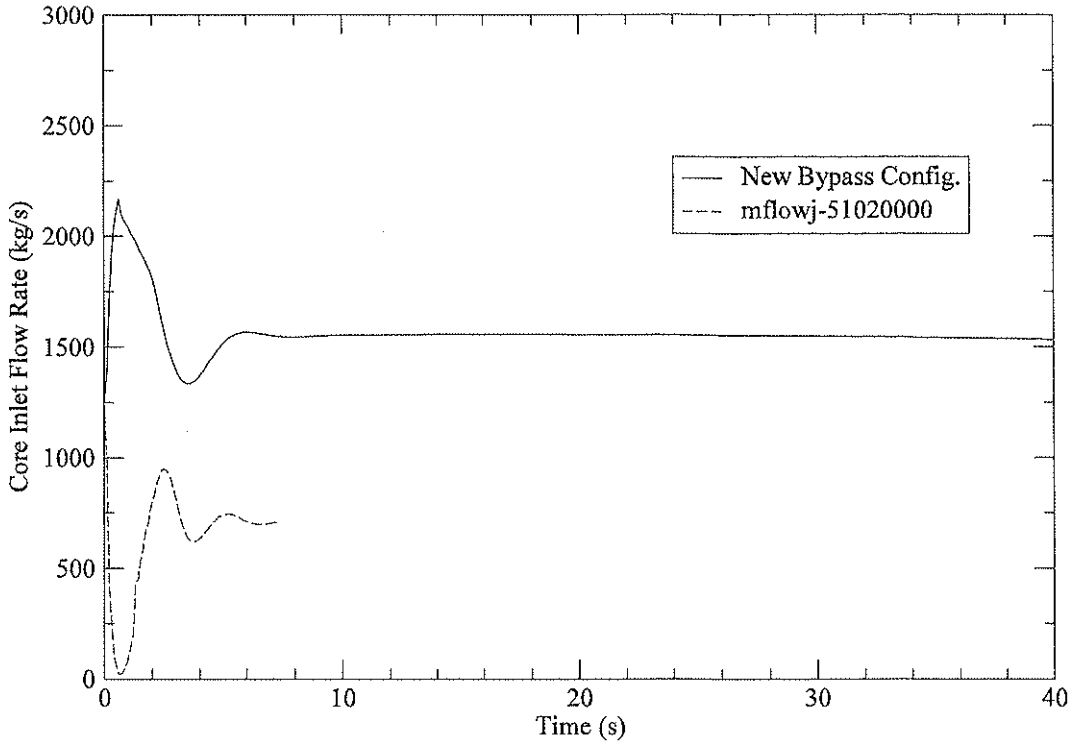

Figure 22. Helium flow at core inlet, old & new bypass line model, loss of load.

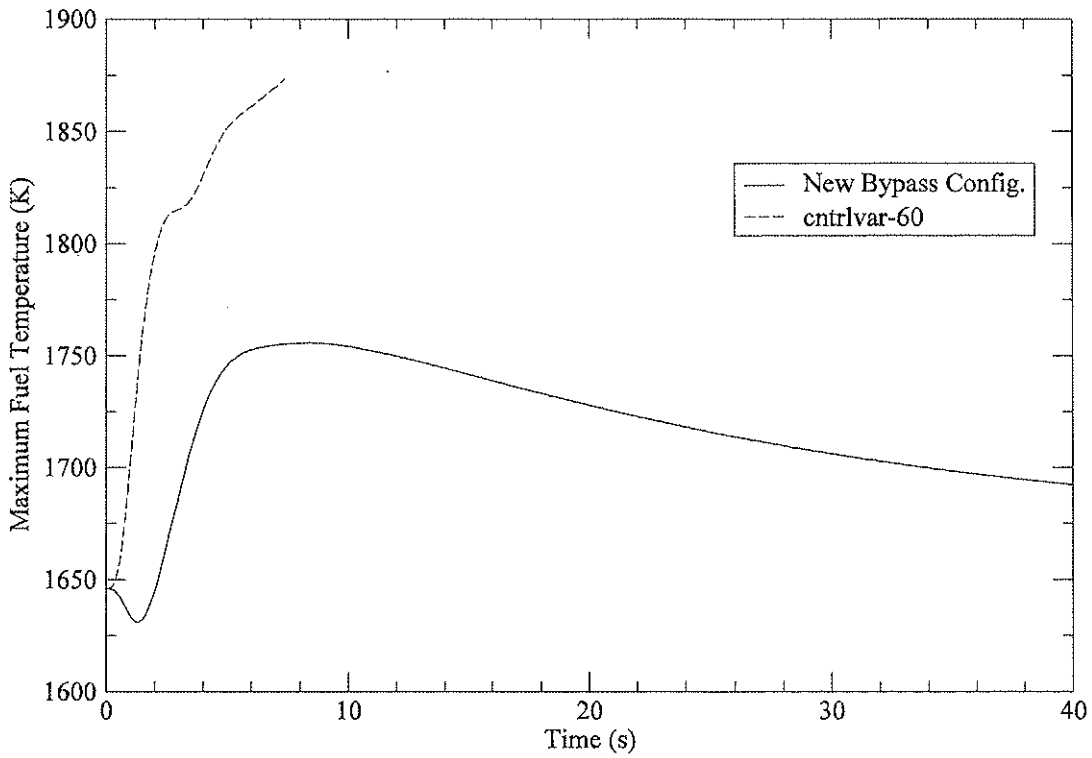

Figure 23. Maximum fuel temperature, old & new bypass line model, loss of load.

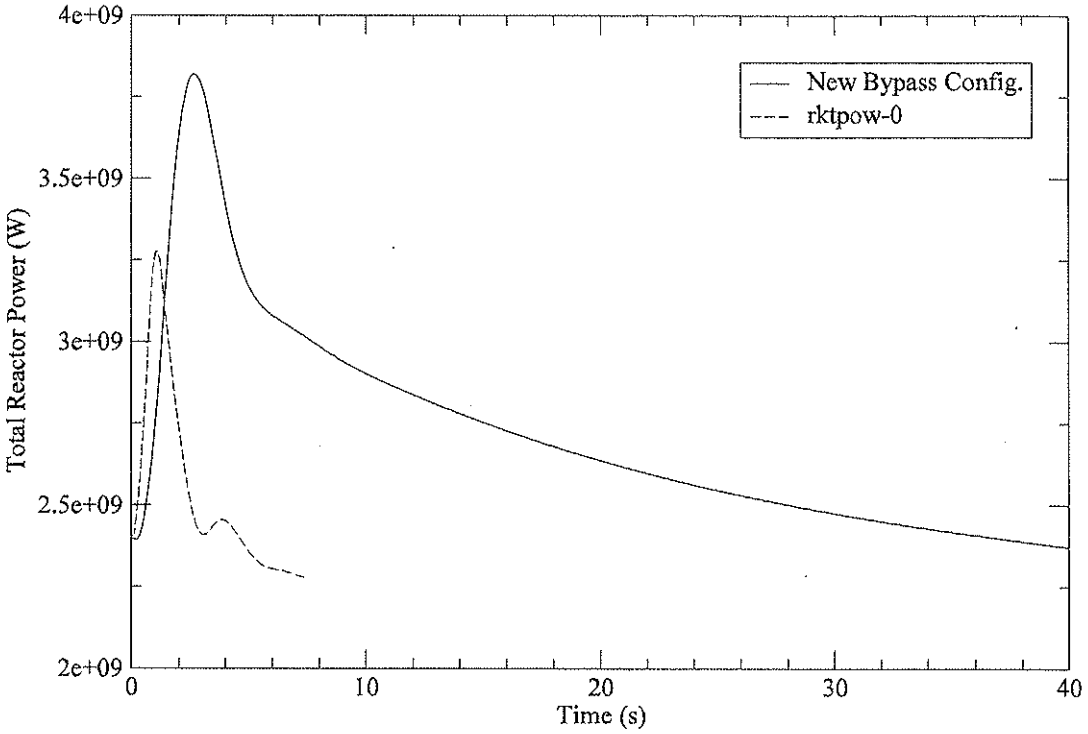

Figure 24. Reactor power, old & new bypass line model, loss of load.

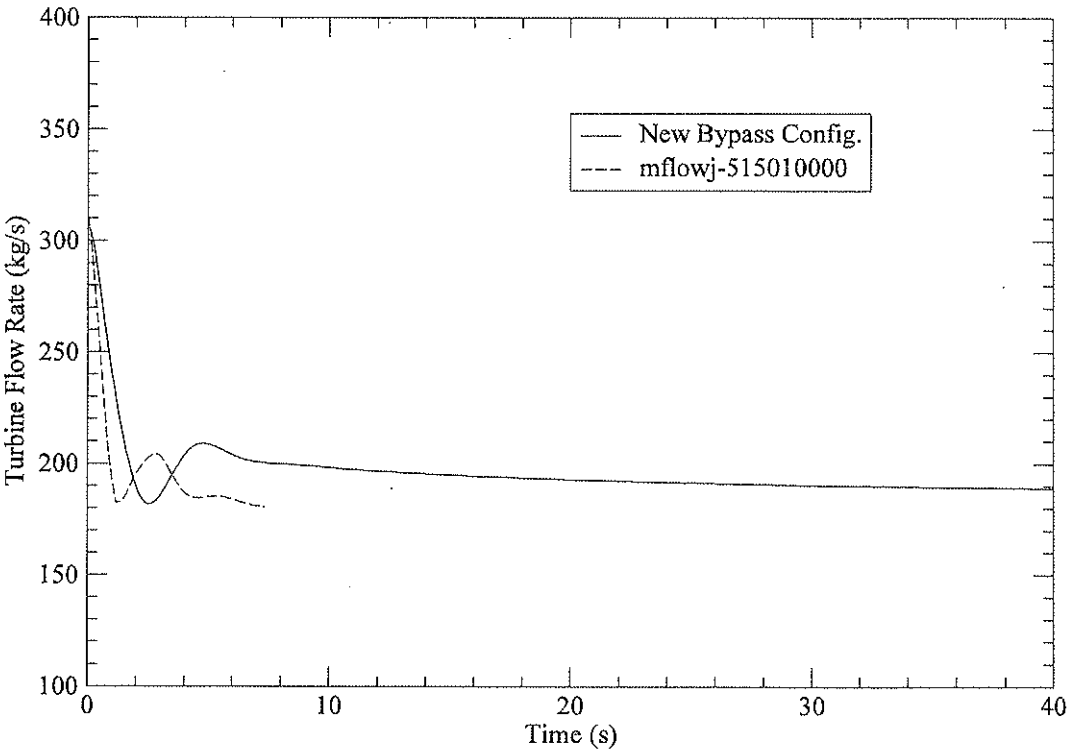

Figure 25. Turbine flow rate, old & new bypass line model, loss of load.

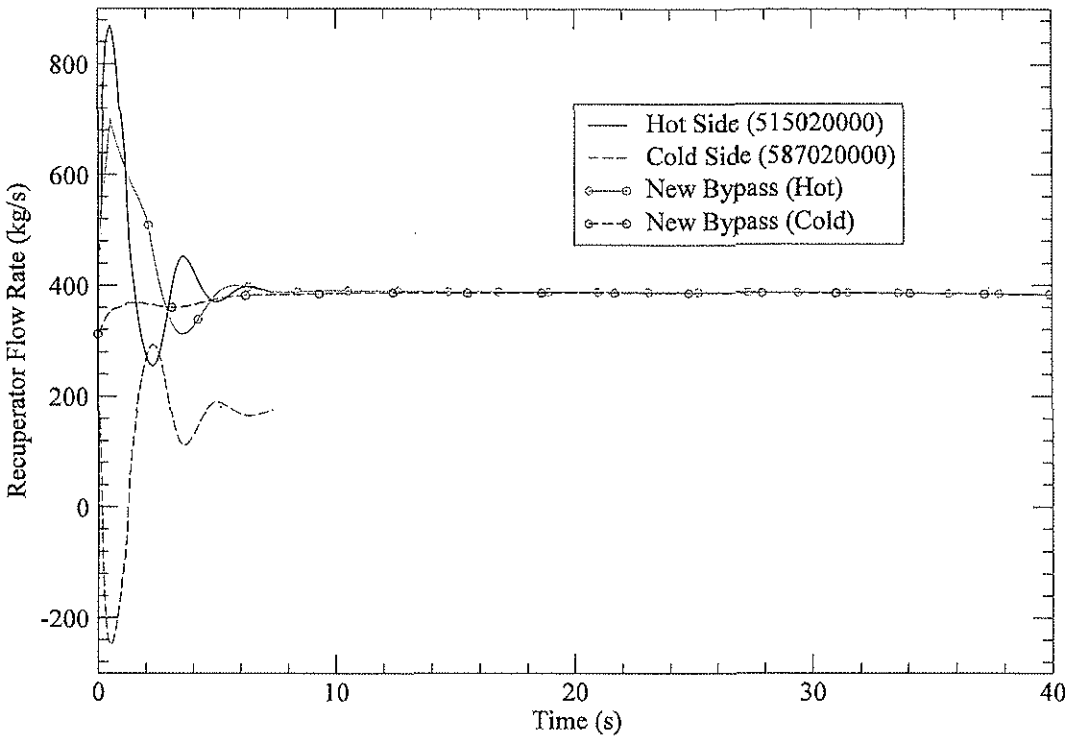

Figure 26. Recuperator flow rate, old & new bypass line model, loss of load.

4.3 Depressurization Accident

This is essentially the same accident as described in Ref. [2] but analyzed with reactivity feedback effect and the new bypass configuration. The accident is initiated by a 10 sq. inch break (0.00645 m^2) and scram is on low system pressure (85% nominal pressure). The increase in reactor power due to positive depressurization reactivity did not raise the power high enough to initiate a scram.

Results for this transient without reactor scram are shown in the following figures. Before the PCU trip at about 150s the slow decrease in system pressure led to a lower helium mass flow rate through the reactor. The increase in fuel temperature was sufficient to introduce a net negative reactivity to lower the reactor power.

The system pressure finally dropped below 85% of nominal system pressure and the PCU was tripped at about 150s. There was a almost step drop in system pressure, causing the reactor power to spike before temperature related negative reactivities kicked in to bring the reactor power on a downward trend. Within roughly 10s the PCU reached quasi-steady condition. The helium flow rate through the reactor was slightly higher than the nominal flow rate because the PCU was running at about 3% above its nominal speed. The core inlet temperature after the PCU trip experienced an initial drop (due to system pressure drop) followed by a step increase. The increase is caused by two factors, decrease in power conversion due to opening of the bypass line, and decrease in cooling water flow to the coolers in the PCU. It is assumed in the modeling of the PCU that upon a trip cooling water to the precooler and the intercooler will be reduced to 5% in 60s.

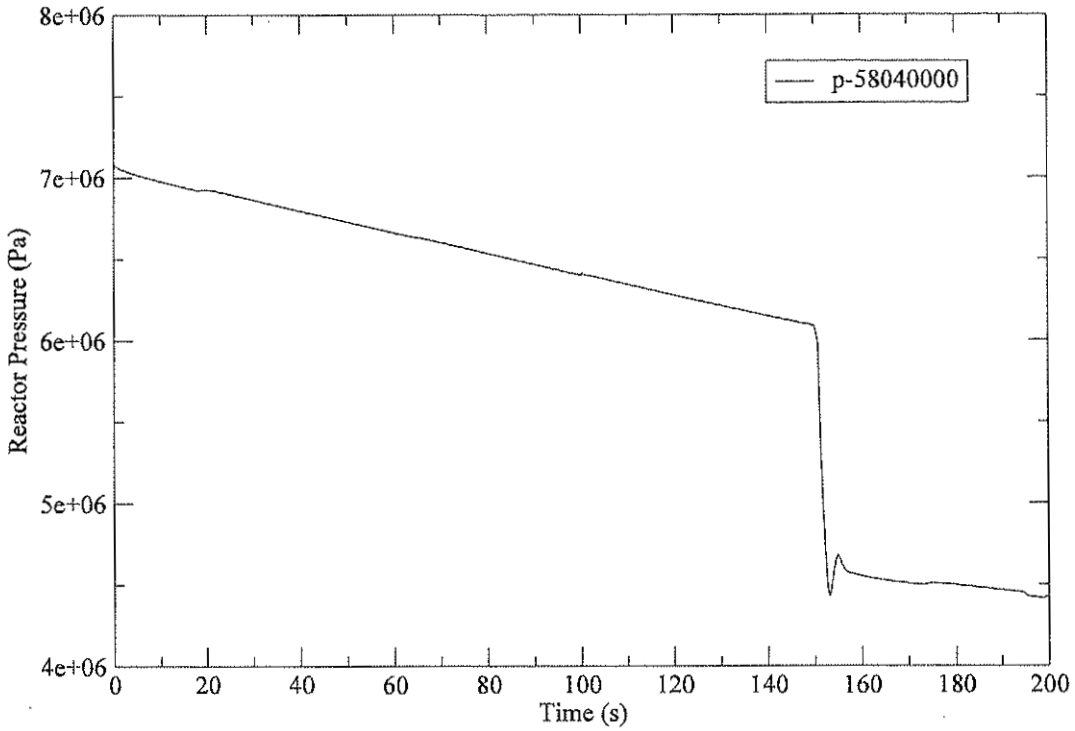

Figure 27. Reactor pressure, depressurization accident.

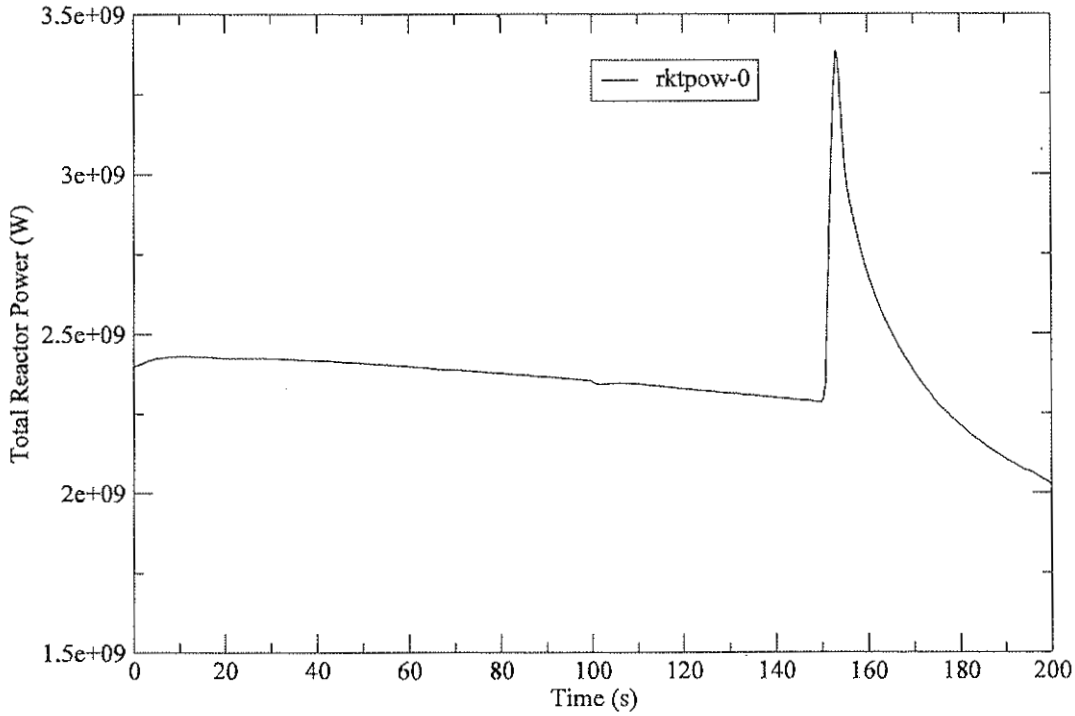

Figure 28. Reactor power, depressurization accident.

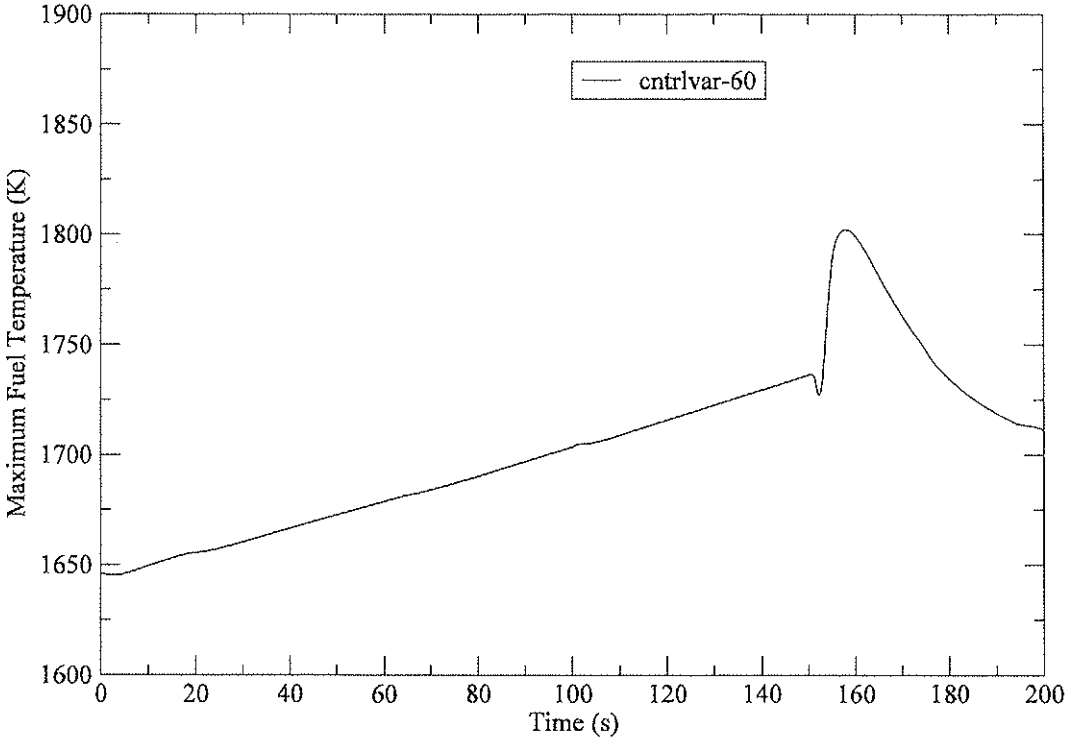

Figure 29. Maximum fuel temperature, depressurization accident.

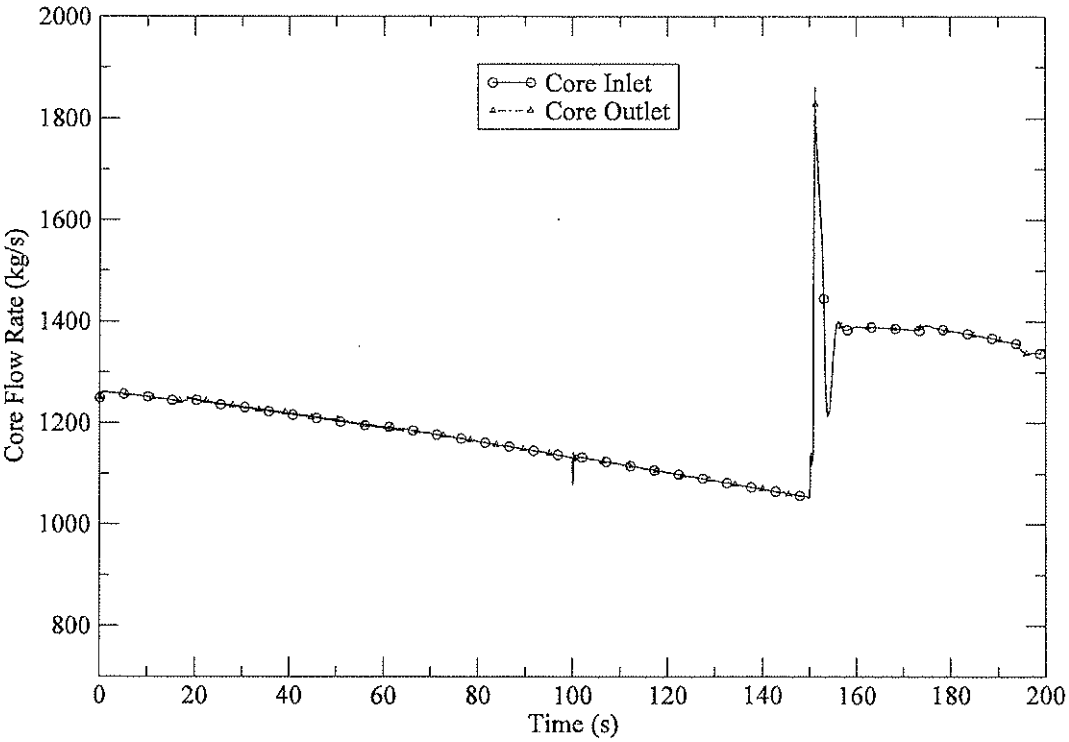

Figure 30. Core flow rates, depressurization accident.

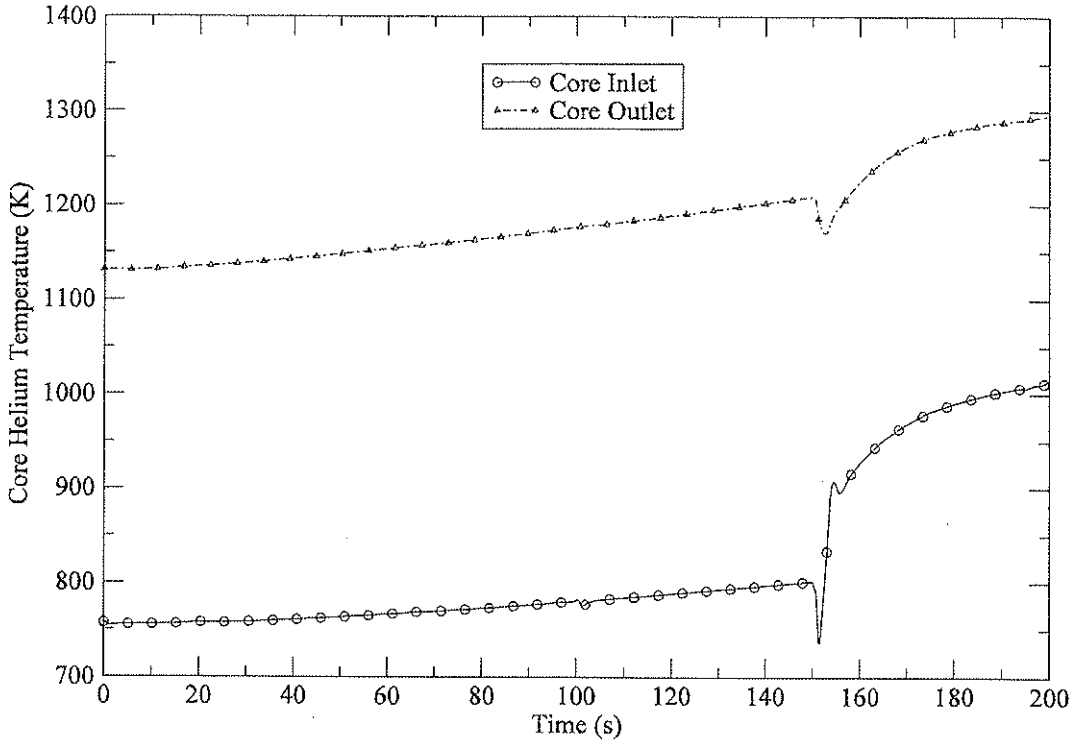

Figure 31. Helium temperature at core inlet and outlet, depressurization accident.

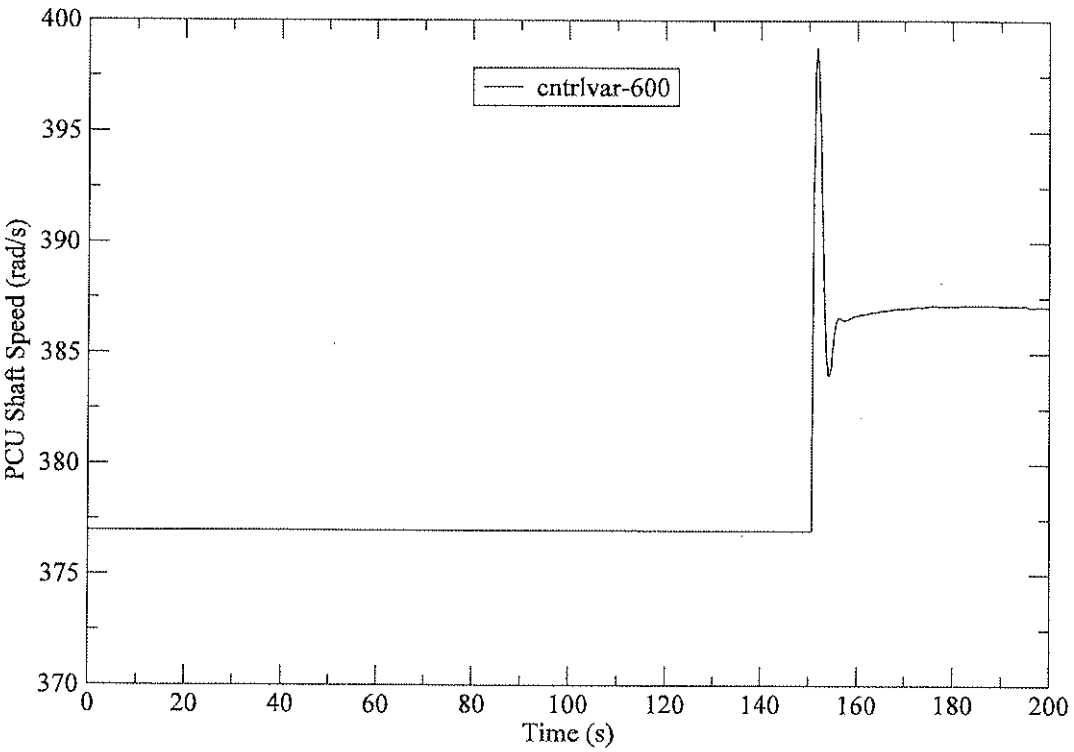

Figure 32. PCU shaft speed, depressurization accident.

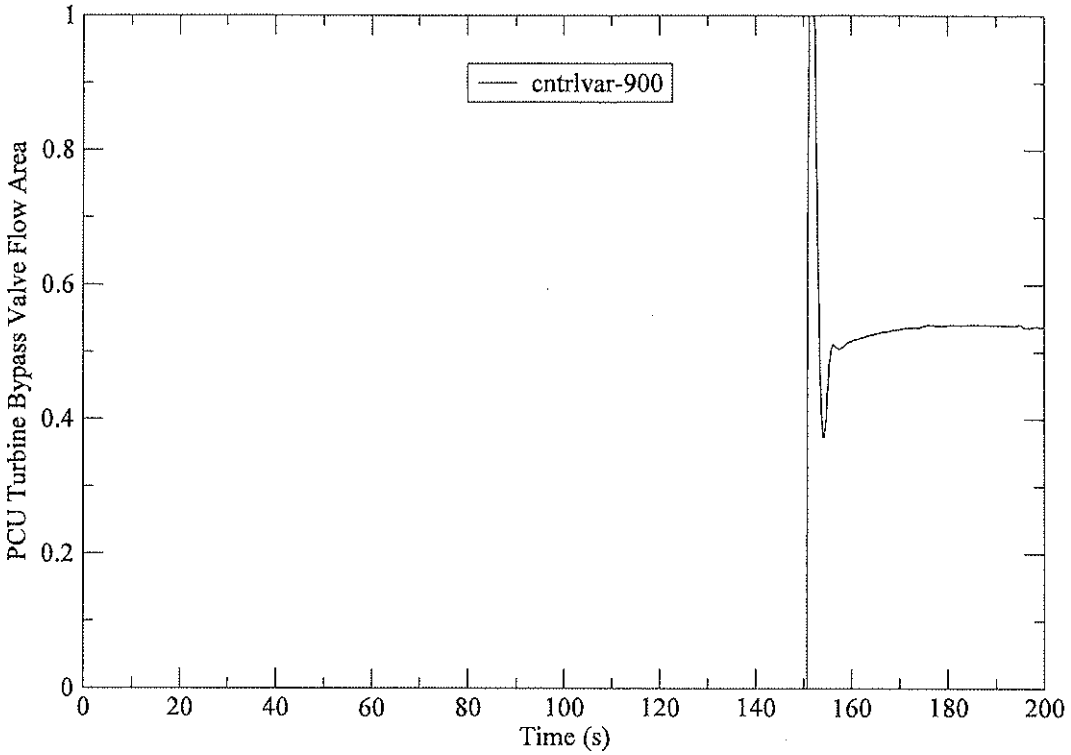

Figure 33. Normalized bypass valve area, depressurization accident.

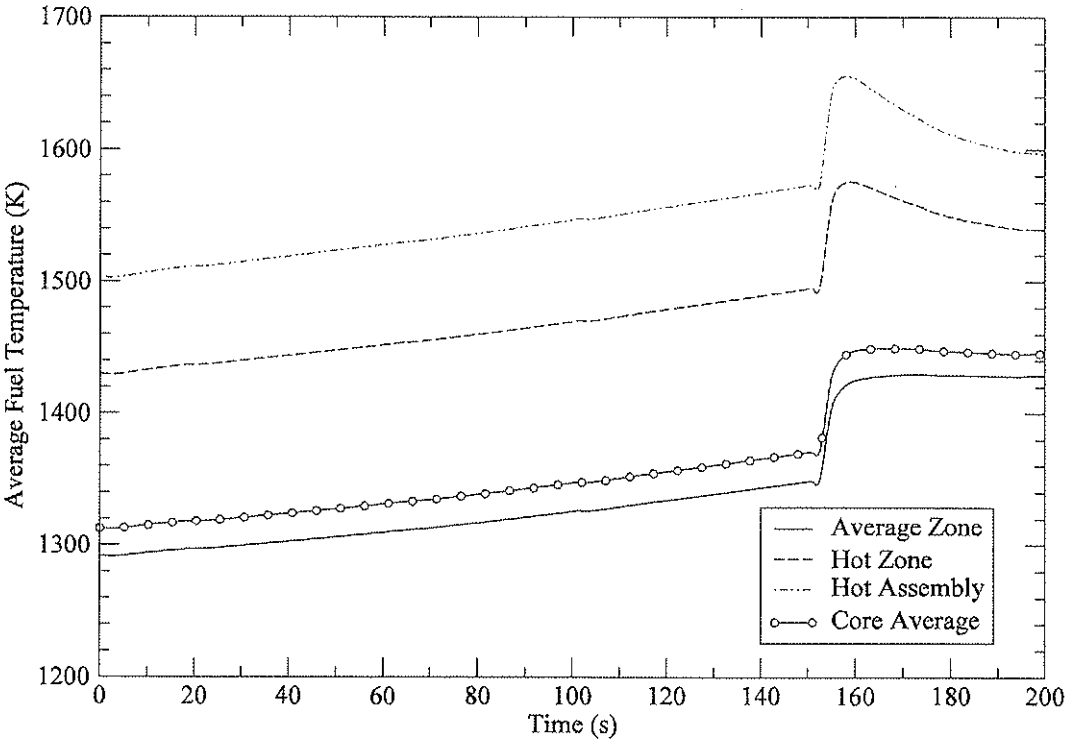

Figure 34, Volume-averaged fuel temperatures, depressurization accident.

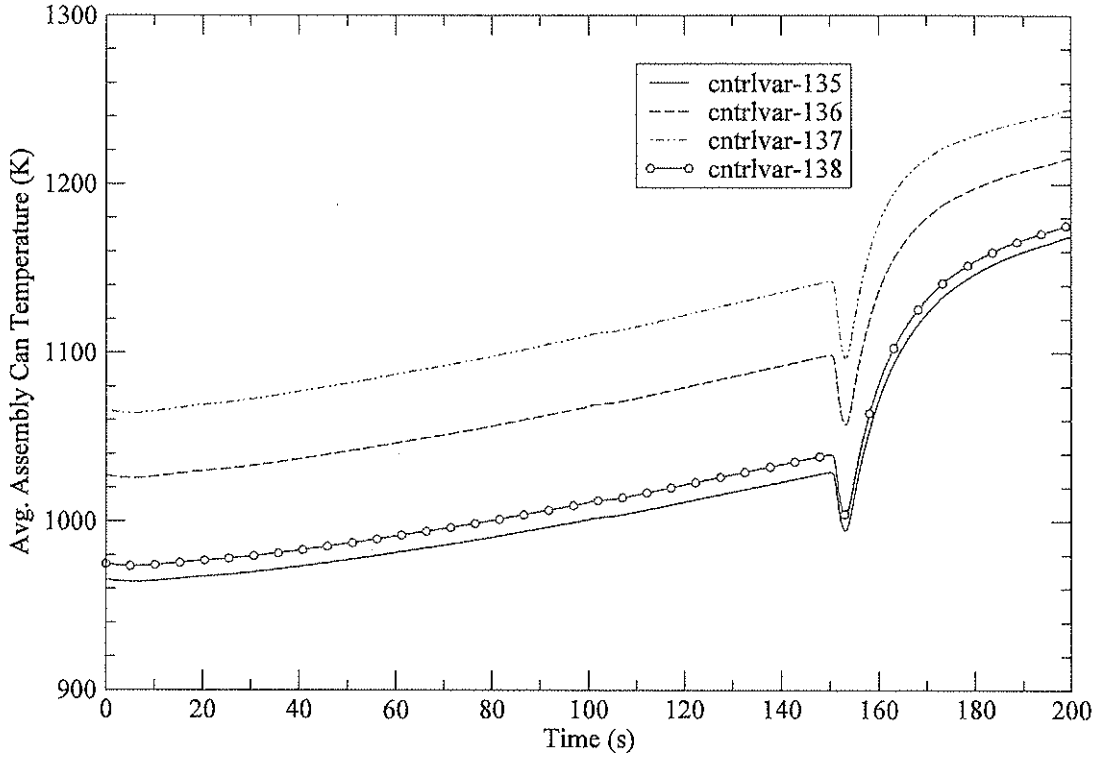

Figure 35. Volume-averaged assembly can temperature, depressurization accident.

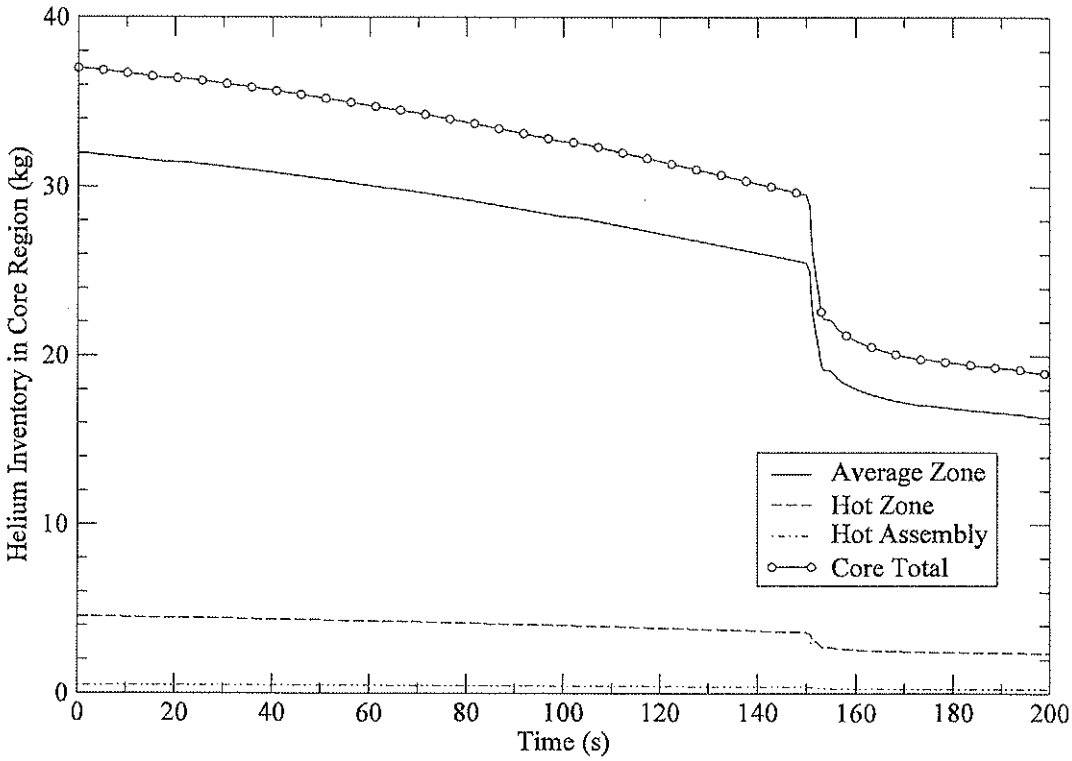

Figure 36. Helium mass in the active core, depressurization accident.

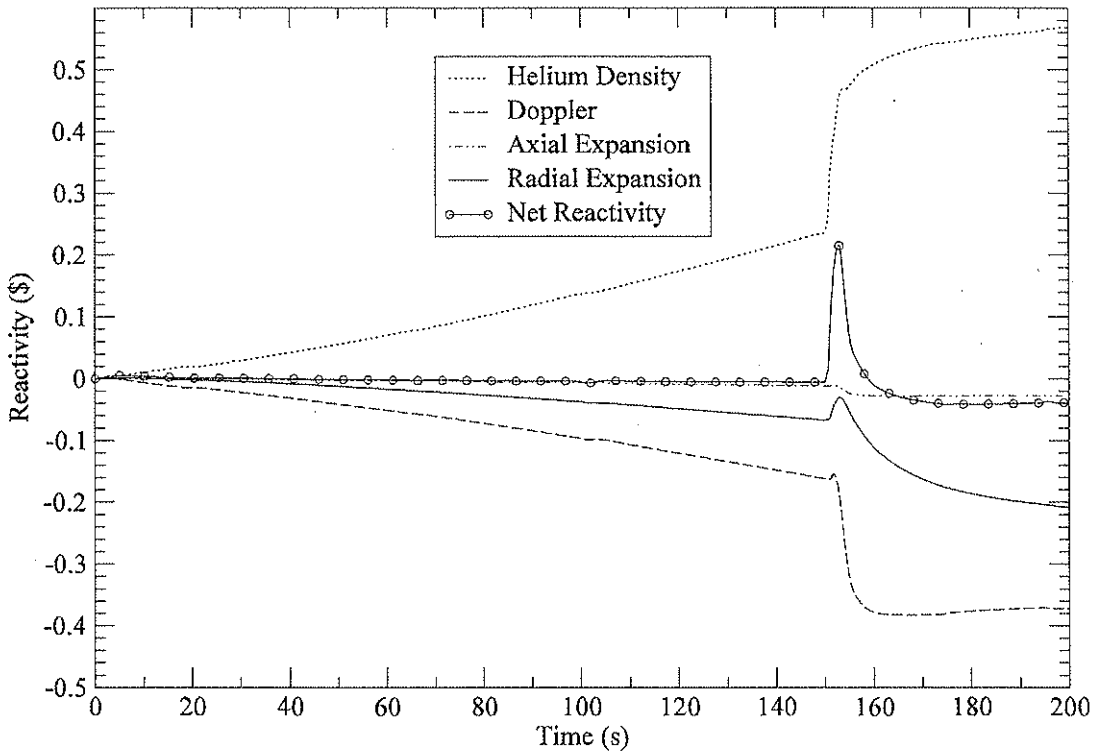

Figure 37. Reactivities, depressurization accident.

With the new bypass line running in parallel with the turbine, the net pressure drop in the PCU is reduced when the bypass line is open. This is the reason for the initial surge in core flow (see Figure 30) when the bypass valve is opened. The effect of this surge in flow on temperature is less significant for the fuel (see Figure 34) than for the assembly can (see Figure 35) because of the higher thermal capacity of the former. It is observed in Figure 37 that at the end of the calculation the sum of the temperature related negative reactivity feedback overcomes the positive feedback from depressurization resulting in a net reactivity that is slightly negative and a reactor power that is declining. Preliminary results from another analysis indicate that the in reactor power continues to decrease between 200s and 500s.

5.0 Conclusions and Path Forward

New input parameters have been implemented in the point kinetics model of RELAP5-3D to model reactivity feedbacks due to changes in system pressure and temperatures in fuel and core structures. Any transient that prompts a PCU trip will cause a decrease in system pressure and an increase in reactor power due to the positive reactivity feedback from depressurization. The increase in reactor power will raise the temperatures of the fuel and other core structures. The temperature increase will introduce negative reactivities that help to mitigate the power increase. However the increase in fuel temperature cannot go unabated because of the 1600°C safety limit. Thus in order for a reactivity transient without scram to be successful, i.e. not to exceed the 1600°C safety limit, there needs to be a delicate balance between reactor power and core cooling (power

and cooling determine the fuel and structure temperatures) while reactivity feedbacks from pressure and temperatures influence the power of the reactor.

The dynamic behavior of the PCU proves to be critical to the system pressure and forced flow cooling of the core. The RELAP5 analyses show that the pressure drop caused by a PCU trip could be reduced by controlling the turbine bypass flow. This is accomplished in the analysis by varying the bypass valve open area according to the amount of over-speed of the PCU shaft. With a modification to the configuration of the turbine bypass line, the analysis demonstrates that core flow is preserved even after the bypass valve is open. The internal recirculation of helium in the PCU is prevented by running the bypass line parallel to the turbine. This new configuration not only effectively prevents over-speeding but also allows full utilization of helium flow to cool the reactor.

Based on the results presented above the following is a list of areas that need further investigation.

- Refine calculation of reactivity coefficients, especially for depressurization.
- Refine models in RELAP5 to represent feedback effects, e.g. implement heat structure model for radial expansion of the core.
- Refine compressor and turbine models in RELAP5 for operations outside the nominal conditions.
- Investigate ways to improve performance of PCU in providing flow and cooling, e.g. control of flow by use of the bypass line, and the role of coolers in an accident.
- Develop strategy for long term cooling in the event of a transient without scram.
- Asymmetric system behavior, e.g. tripping of just one of the four PCUs.

6.0 References

[1] Farmer, M. et al., "Generation IV Nuclear Energy System Initiative Pin Core Subassembly Design," ANL-GENIV-070, April 2006..

[2] Cheng, L. and Ludewig, H., "Combined Active/Passive Decay Heat Removal Approach for the 2400MWt Gas-Cooled Fast Reactor," DOE GEN-IV program report, BNL-GFR-2006-001, March 31, 2006.

[3] Cheng, L. and Ludewig, H., "2400MWt Gas-Cooled Fast Reactor DHR Studies Status Update," DOE GEN-IV program report, BNL-GFR-2006-002, August 31, 2006.

[4] Personal communication with Tom Wei of ANL, e-mail with attachment, dated March 27, 2007.

[5] Meyer, M., "Properties of (U,Pu)C and (U,Pu)N for use as Gas-cooled Fast Reactor Fuels," Rev. 0, ANL, October 27, 2003.

[6] "Thermal Expansion Coefficient of Hexoloy SA Silicon Carbide," Saint-Gobain Ceramics, http://www.hexoloy.com.